AWARD NUMBER: W81XWH-17-1-0029

TITLE: Adenosine Blockade with Radiotherapy to enhance responses of breast cancer to immune checkpoint inhibitors

PRINCIPAL INVESTIGATOR: Erik Wennerberg

CONTRACTING ORGANIZATION: Weill Cornell Medicine

REPORT DATE: May 2020

TYPE OF REPORT: Final report

PREPARED FOR: U.S. Army Medical Research and Development Command
Fort Detrick, Maryland 21702-5012

REPORT DOCUMENTATION PAGE

Form Approved
OMB No. 0704-0188

1. REPORT DATE	**2. REPORT TYPE**	**3. DATES COVERED**
May 2020	Final Report	02/01/2017 - 01/31/2020

4. TITLE AND SUBTITLE
Adenosine Blockade with Radiotherapy to enhance responses

of breast cancer to immune checkpoint inhibitors

5a. CONTRACT NUMBER

5b. GRANT NUMBER
W81XWH-17-1-0029

5c. PROGRAM ELEMENT NUMBER

6. AUTHOR(S)
Erik Wennerberg

E-Mail: erw2010@med.cornell.edu

5d. PROJECT NUMBER

5e. TASK NUMBER

5f. WORK UNIT NUMBER

7. PERFORMING ORGANIZATION NAME(S) AND ADDRESS(ES)

Weill Cornell Medicine
1300 York Avenue, E-209
New York, NY 10065

8. PERFORMING ORGANIZATION REPORT

9. SPONSORING / MONITORING AGENCY NAME(S) AND ADDRESS(ES)

U.S. Army Medical Research and Development Command
Fort Detrick, Maryland 21702-5012

10. SPONSOR/MONITOR'S ACRONYM(S)

11. SPONSOR/MONITOR'S REPORT NUMBER(S)

12. DISTRIBUTION / AVAILABILITY STATEMENT

Approved for Public Release; Distribution Unlimited

13. SUPPLEMENTARY NOTES

14. ABSTRACT

A majority of patients with advanced breast cancer are currently non-responsive to immune checkpoint blockade (ICB) due to a lack of intratumoral CD8 T cell infiltration. Localized radiation therapy (RT) can be used as a spark to trigger systemic immunity and render patients susceptible to ICB, mediating abscopal effects (outside of the irradiated field) and occasionally tumor clearance and long-lasting immune memory. The ability of the host to mount tumor-specific CD8 T cell responses is highly dependent on tumor infiltration of dendritic cells (DCs), particularly conventional type I DCs (cDC1). However, following RT, adenosine (ADO) accumulation in the tumor microenvironment (TME) acts to suppress both DC subsets and effector CD8 T cells thus limiting the immunogenic effect of RT. During the research project, we have described that high doses of RT induces a rapid increase in ADO levels in tumors and causes upregulation of key enzymes involved in generation of ADO on tumor cells. Moreover, we have shown that ADO-blockade by anti-CD73 antibody therapy promotes infiltration of cDC1 cells in irradiated tumors. Importantly, we demonstrate that ADO-blockade promotes synergy between RT and ICB to induce systemic immune responses in mouse models of metastatic breast cancer.

15. SUBJECT TERMS Breast cancer, Immune checkpoint blockade (ICB), Radiation therapy (RT), Abscopal effect, Dendritic cells (DCs), Conventional type I DCs (cDC1), CD8 T cells, Tumor microenvironment (TME), Adenosine triphosphate (ATP, Adenosine (ADO)					
16. SECURITY CLASSIFICATION OF:			**17. LIMITATION OF ABSTRACT**	**18. NUMBER OF PAGES**	**19a. NAME OF RESPONSIBLE PERSON** USAMRMC
a. REPORT Unclassified	**b. ABSTRACT** Unclassified	**c. THIS PAGE** Unclassified	Unclassified	50	**19b. TELEPHONE NUMBER** *(include area code)*

Standard Form 298 (Rev. 8-98)
Prescribed by ANSI Std. Z39.18

TABLE OF CONTENTS

Annual Report/Final report

Department of Defense Breakthrough Fellowship Award

Project title: *Adenosine Blockade with Radiotherapy to enhance responses of breast cancer to immune checkpoint inhibitors.*

Award number: W81XWH-17-1-0029

Reporting period: 1 Feb 2017 - 31 Jan 2020

1. INTRODUCTION

A majority of patients with advanced breast cancer are non-responsive to immune checkpoint blockade (ICB) due to a lack of CD8 T cell infiltration. Recently, findings from pre-clinical mouse models and clinical trials have shown that localized radiation therapy (RT), can act as a spark triggering systemic immunity and rendering patients susceptible to ICB. Immune responses arising from the synergy between RT and ICB can mediate abscopal effects (anti-tumor effects outside of the radiation field) and occasionally tumor clearance and long-lasting immunological memory. In this way, RT works as an *in situ* tumor vaccination The ability of patients to mount tumor-specific CD8 T cell responses is dependent on tumor infiltration of dendritic cells (DCs), particularly conventional type I DCs (cDC1) which are superior at presenting tumor-derived antigens to CD8 T cells. Following RT, extracellular ATP accumulates in the tumor, constituting one of the essential danger signals that recruit and activate cDC1s. However, ATP is rapidly degraded by ectoenzymes CD39 and CD73 in the tumor microenvironment (TME) into adenosine (ADO) which suppresses both DCs and effector CD8 T cells thus counteracting the immunogenic effect of RT. Recently, it has been described that ADO can also be generated via CD38 and CD203a-mediated hydrolysis of NAD+.

This research project has discerned the mechanism by which ADO generation in irradiated tumors affects the radiation-induced immune response, specifically the role of tumor infiltration and activation of cDC1. The ultimate goal was to test the hypothesis that patients suffering from poorly immunogenic breast cancer, can benefit from treatment with ADO blockade to become responsive to ICB.

2. KEYWORDS

Breast cancer
Immune checkpoint blockade (ICB)
Radiation therapy (RT)
Abscopal effect
Dendritic cells (DCs)
Conventional type I DCs (cDC1)
CD8 T cells
Tumor microenvironment (TME)
Adenosine triphosphate (ATP)
Adenosine (ADO)

3. ACCOMPLISHMENTS

What were the major goals of the project?

Specific Aim 1: Determine the effect of ADO blockade in combination with RT on DC activation and generation of tumor-specific T cells

> ***Major Goal 1 (Months 1-12):*** Determine the effect of different RT doses and fractionation regimen on ADO release and immunogenicity
>
> **Major Goal 2 (Months 12-24):** Evaluate tumor progression and immune cell infiltration of combined RT and ADO-blockade in vivo

Specific Aim 2: Determine if ADO blockade in combination with RT enhances the anti-tumor effect of immune checkpoint blockade in breast cancer

> **Major Goal 1 (Months 18-30):** Evaluate the immunogenic and anti-tumor effect of RT + ADO-blockade in combination with anti-CTLA-4 treatment
>
> **Major Goal 2 (Months 25-36):** Evaluate the immunogenic and anti-tumor effect of RT + ADO-blockade in combination with anti-PD-1 treatment

What was accomplished under these goals?

Specific Aim 1:
Determine the effect of ADO blockade in combination with RT on DC activation and generation of tumor-specific T cells

Major Goal 1 (Months 1-12):
Determine the effect of different RT doses and fractionation regimens on ADO release and immunogenicity

Major activities:
We sought to determine how RT modulates the adenosinergic signaling pathway. To this end we treated mice bearing ectopically implanted flank mammary tumors (TSA) with increasing doses of RT and harvested tumors after 24 hours for measurement of adenosine abundance by mass spectrometry (Figure 1A). TSA tumors were also harvested for assessment of the ADO-generating enzymes CD39 and CD73 in whole tumor homogenates. Tumors were harvested 24 hours after RT, homogenized and analyzed by flow cytometry for CD39 and CD73 expression (Figure B-C). In addition, expression of enzymes from the non-canonical pathway of ADO-generation (CD38, CD203a and CD73) was assessed in vitro in mouse mammary tumor cells (TSA and 4T1 cell lines) and CD38 and CD73 expression was assessed on human breast cancer cell lines (MDA-MB-231 and 4175TR) treated with different RT doses and fractionation regimens (Figure 2D-F).

Specific objectives:

a. Determine the effect of RT on generation of ADO in mouse tumors.

b. Assess whether ADO-generating enzymes are modulated by RT

Significant results:

a. Mass spectrometry analysis of TSA tumors harvested 24 hours after local RT treatment revealed that significantly higher levels of ADO abundance

in tumors treated with 20Gy RT compared to mock-treated tumors (Figure 1A).

b. Flow cytometry analysis of CD39 and CD73 in TSA tumors revealed that CD39 expression was detected only on immune cells (CD45+) while it was not expressed on CD45- cells which includes tumor cells (Figure 1B). CD73 was expressed on both CD45+ cells and CD45- cells while there was a significant increase in expression in irradiated tumors only in the CD45- cells (Figure 1C). Increased surface expression of CD73 as well as of CD38 and CD203a on irradiated TSA and 4T1 tumor cells 24 hours following RT was confirmed in in vitro experiments (Figure 1D). Surface expression of CD38 and CD73 was increased on MDA-MB-231 cells (Figure 2E) and on 4175TR cells (Figure 2F) with the strongest upregulation observed in cells treated with 8Gyx3 RT.

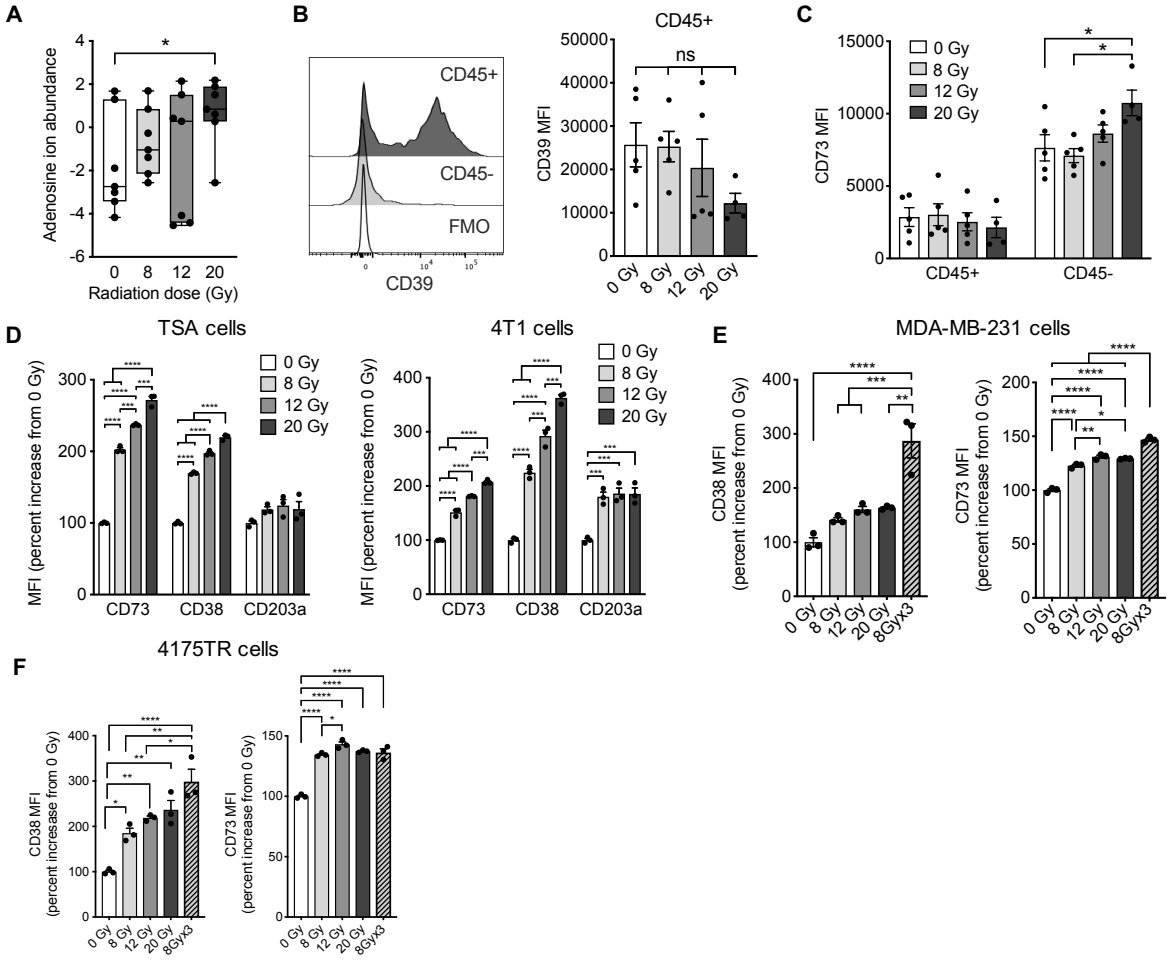

Figure 1. Mice bearing subcutaneous TSA flank tumors were treated with focal RT at different doses, as indicated. Twenty-four hours after RT, tumors were excised and either snap-frozen for analysis of adenosine concentration by liquid-chromatography/mass spectrometry (LC/MS) (n=7 per group) (**A**), or enzymatically digested into single cell suspension for flow cytometry analysis (n=4-5 per group) (**B-C**). (**A**) Adenosine ion abundance, Data was normalized to median and Log2 transformed. Plot shows median values and interquartile range. *p<0.05, Welch's t-test. The experiment was performed twice with similar results. (**B**) Surface expression of CD39 on CD45+ and CD45- cells. Representative histograms (left panel) and mean fluorescence intensity (MFI) on CD45+ cells (right panel). (**C**) Surface expression of CD73 on CD45+ and CD45- cells. TSA and 4T1 tumor cells were treated with single doses of 0, 8, 12 and 20Gy RT and analyzed 24 hours later for ectoenzyme surface expression by flow cytometry. (**D**) Expression of CD73, CD38 and CD203a on TSA tumor cells (left panel) and on 4T1 tumor cells (right panel) 24 hours after irradiation with the indicated doses. Bar graphs show percent change in MFI compared to mock-treated cells (0Gy). Expression of CD73 and CD38 on human breast cancer cells (**E**) MDA-MB-231 and (**F**) 4175TR 24 hours after irradiation with the indicated doses. Bar graphs show percent change in MFI compared to mock-treated cells (0Gy). ANOVA was used to compare changes in MFI across treatment groups followed by pairwise comparisons using Tukey's method *p<0.05, **p<0.01, ***p<0.001, ****p<0.0001. All data shows mean±s.e.m.

Milestone (month 12):
Determination of optimal RT regimen for combination with ADO-blockade

Status: Completed. We established that ADO abundance is increased in RT-treated tumors in a dose-dependent fashion and that ADO-generating enzymes are upregulated on irradiated tumors cells.

Major Goal 2 (Months 12-24): Evaluate tumor progression and immune cell infiltration of combined RT and ADO-blockade in vivo

Major activities:
We wanted to determine whether mammary tumors are sensitized to the anti-tumor effect of RT by concomitant treatment with ADO-blockade and how RT-mediated infiltration of tumor infiltrating DCs and T cells is impacted by ADO-blockade. We administered ADO-blockade by anti-CD73 blocking antibodies concomitantly with local tumor irradiation (20 Gy) and followed the mice for

tumor progression and long-term survival. Some mice were sacrificed on day 6 after RT to determine infiltration of tumors by T cells and DCs (Experiment layout in Figure 2A). Further, we sought to determine whether the synergy between ADO-blockade and RT is due to blockade of CD73 on the cancer cells and/or the tumor stroma. To this end TSA cells were transduced with a doxycycline-inducible shRNA construct targeting CD73 (TSA^{shCD73}). After confirming effective knockdown (Figure 2D), TSA^{shCD73} and TSA cells expressing a non-silencing construct (TSA^{shNS}) were implanted into mice. Six days later mice were given doxycycline to induce CD73 knockdown followed by treatment with 20Gy RT and mice were followed for tumor progression and survival (Experiment layout in Figure 2E).

We assessed the effect of ADO-blockade on tumor infiltration of T cells and DCs in RT treated tumors by flow cytometry where we determined the frequency of cDC1s among total DCs and their activation state by staining for CD86 surface expression. In addition, we determined the percentage of CD8 T cells and regulatory T cells (Tregs) among total T cells and assessed CD8 T cell activation state by staining for CD69 surface expression (Figure 3).

In a time-course study, we tested whether also the absolute number of cDC1 cells was increased in tumors treated with RT and ADO-blockade (Figure 4 A-B) and assessed by fluorescence microscopy the location of cDC1s and T cells within the tumor (Figure 4C).

In order to determine the importance of cDC1 infiltration in RT-treated tumors induced by ADO-blockade we challenged mice that are deficient in developing cDC1s (BATF3-/- mice) with TSA tumors, treated them with RT and ADO-blockade (as in Figure 2A) and assessed the tumor progression and infiltration of CD8 T cells (Figure 5).

Further, in order to specifically test whether ADO-blockade could improve the homing and infiltration of cDC1s to irradiated tumors, we designed an experiment where cDC1s, isolated from immunocompetent wild type mice, were labeled with a fluorescent dye (CFSE) and adoptively transferred by tail vein injection to $BATF3^{-/-}$ mice bearing TSA flank tumors treated with 20Gy RT with or without prior ADO-blockade (Experiment layout in Figure 6A). 48 hours after adoptive transfer we analyzed the tumors for cDC1 infiltration by flow cytometry staining (Figure 6B).

Previous findings have shown that RT delivered at 8Gyx3 induces cDC1 tumor infiltration by triggering tumor production of IFN type I via cGAS/STING signaling (Vanpouille-Box, Nat Commun, 2017). We hypothesized that RT-induced ATP release in tumors constitutes an alternative pathway of cDC1 recruitment and infiltration to tumors while conversion into ADO abrogates this process. Thus, ADO-blockade could potentiate the ability of RT to induce cDC1 tumor infiltration. To test our hypothesis, with treated tumors with dysfunctional IFN type I signaling (TSA tumors transduced with an shRNA silencing expression of cGAS (TSA^{shcGAS})) with 8Gyx3 RT and assessed infiltration of cDC1 cells by flow cytometry. Tumors transduced with a non-silencing shRNA (TSA^{shNS}) were used as controls (Figure 7A).

Moreover, we wanted to assess whether the ability of ADO-blockade to promote tumor infiltration of adoptively transferred cDC1s to RT-treated tumors is independent of IFN type I signaling. To this end, we isolated cDC1s from mice that are deficient in the IFN type I receptor (IFNAR-/-) or from wild type (WT) mice, labeled them with a fluorescent dye (CFSE) and adoptively transferred them into wild type mice treated with 20Gy RT or 8Gyx3 RT with or without ADO-blockade. Tumors were analyzed for infiltration of CFSE-labeled cDC1s 48 hours after adoptive transfer (Figure 7B).

Specific objectives:

a. Determine if ADO-blockade by anti-CD73 antibody treatment and/or knockdown of CD73 expression on cancer cells improves the tumor response to RT

b. Assess tumor infiltration of DCs and T cells in mice treated with ADO-blockade and RT

c. Determine whether ADO-blockade in combination with RT increases the density of cDC1 cells within tumors and confirm cDC1 tumor infiltration in tumor tissue

d. Assess the importance of cDC1 cells for the synergy between ADO-blockade synergy and RT

e. Investigate whether ADO-blockade can improve homing and infiltration of adoptively transferred cDC1s to irradiated tumors

f. Assess whether the synergistic effect of RT and ADO-blockade to promote tumor-infiltration of cDC1s works independently of IFN type I signaling.

Significant results:

a. ADO-blockade by treatment with CD73 blocking antibodies had no significant effect on tumor progression and survival in non-irradiated mice. In combination with RT, ADO-blockade enhanced significantly tumor response and extended mice survival, with 2/7 mice showing complete tumor regression (Figure 2B-C). To determine whether the activity of the combination treatment was due to ADO-blockade on the cancer cells and/or the tumor stroma, TSA cells were transduced with a doxycycline-inducible shRNA construct targeting CD73 (TSA^{shCD73}). After confirming effective knockdown (Fig 2D), TSA^{shCD73} and TSA cells expressing a non-silencing construct (TSA^{shNS}) were implanted into mice. Six days later mice were given doxycycline to induce CD73 knockdown followed by treatment with 20Gy RT (Figure 2E). In the absence of radiation, CD73 knockdown did not affect tumor growth, whereas in mice treated with 20 Gy RT it improved tumor response to the same extent as antibody-mediated blockade of CD73 in mice bearing TSA^{shNS} tumors (Figure 2F-G). Addition of anti-CD73 antibody to mice bearing TSA^{shCD73} and treated with RT did not further improve tumor control or mice survival (Fig 2F-G), indicating that CD73 expressed by the cancer cells is the critical target limiting the response to RT.

b. Analysis of intratumoral T cells and DCs revealed that ADO-blockade by anti-CD73 antibody treatment by itself did not have any effect, but it increased the cDC1 subset (identified by CD8a expression) of intratumoral DCs and their expression of the maturation marker CD86 when used with 20Gy RT (Figure 3A-B). Analysis of the T cell compartment revealed an increase in CD8 T cells in tumors of mice treated with 20Gy and CD73-blockade (Figure 3C). Expression of CD69, a marker of T cell activation and tissue-resident differentiation, was enhanced in the CD8 T cells present within irradiated tumors, and further enhanced by CD73-blockade (Figure 3D). Treg cells were significantly increased by 20Gy but this increase was abrogated by CD73-blockade (Figure 3E). The ratio of CD8/Tregs cells, was significantly increased only in the tumor of mice treated with RT and CD73-blockade (Figure 3F).

c. We observed an increase in absolute numbers of cDC1 cells per gram of tumor following treatment with combined RT and CD73-blockade reaching statistical significance compared with untreated tumors on day 6 after tumor irradiation. (Figure 4B). We confirmed by immunofluorescence staining that cDC1s are infiltrating tumors treated with RT and ADO-blockade and that DCs and T cells are interacting within the tumor tissue (Figure 4C-D).

d. The synergy between 20Gy RT and CD73-blockade was completely abrogated in Batf3-/- mice (Figure 5A). Consistently with the inability of these mice to activate anti-tumor CD8 T cells, the intratumoral CD8/Treg cell ratio was not increased in Batf3$^{-/-}$ mice treated with 20Gy and CD73-blockade (Figure 5B). The modest increase in expression of CD69 by CD8 T cells induced by RT was still observed, but it was not further increased by CD73-blockade (Figure 5C), indicating that the effects of CD73-blockade are dependent on cDC1.

e. CD73-blockade significantly enhanced cDC1 infiltration in irradiated but not untreated tumors (Figure 6B). These results indicate that cDC1 homing to TSA tumors requires chemotactic and/or survival signals induced by RT together with blockade of adenosine generation.

f. We observed that 8GyX3 RT increased cDC1 in TSA^{shNS} tumors but not in TSA^{shcGAS} tumors. Addition of CD73-blockade marginally increased cDC1 in irradiated TSA^{shNS} tumors. In contrast, in mice bearing irradiated TSA^{shcGAS} tumors CD73-blockade restored RT-induced cDC1 recruitment (Figure 7A).

In adoptive transfer experiments, in accordance with previous findings, WT cDC1 infiltrated to a higher degree tumors treated with 8GyX3 than 20Gy RT (Figure 2B, left panel). In contrast, homing of Ifnar$^{-/-}$ cDC1 to tumors treated with 8GyX3 RT was not different from tumor treated with 20Gy RT (Figure 2B, right panel). Whereas CD73-blockade did not further increase infiltration of WT cDC1 to tumors treated with 8GyX3, it restored infiltration of WT cDC1 to tumors treated with 20Gy (Figure 2B, left panel). Importantly, it also restored infiltration of the Ifnar$^{-/-}$ cDC1 to tumors treated with either 8GyX3 RT or 20Gy RT (Figure 2B, right panel).

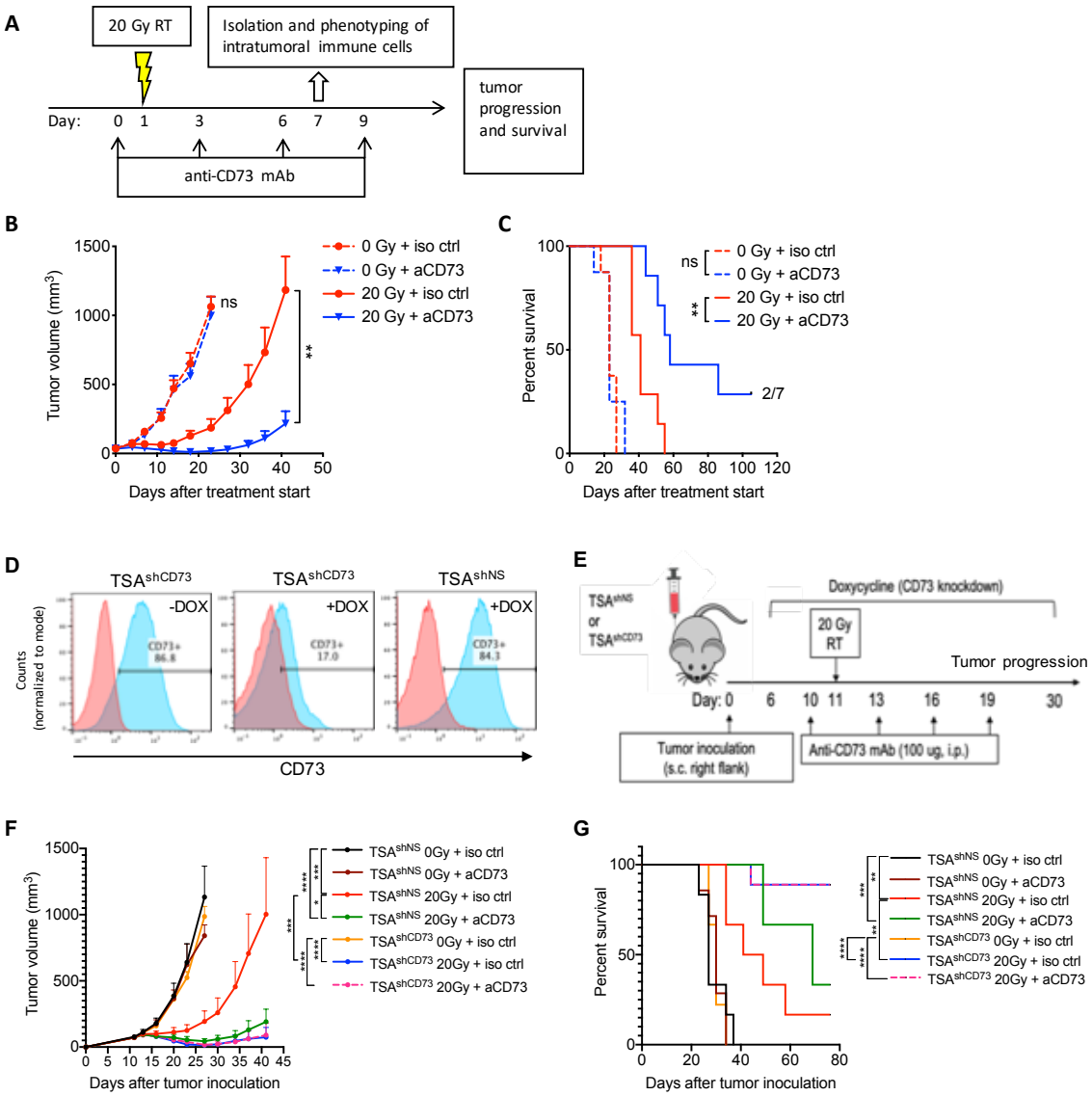

Figure 2. (**A**) Tumor treatment schema. Mice bearing TSA tumors were treated with 20Gy RT and/or anti-CD73 (aCD73, Clone: TY/23, 100µg i.p.) monoclonal antibody (mAb) or isotype control antibody (iso ctrl, Clone: 2A3,100 µg, i.p.), as indicated. Some mice were sacrificed one day after the third antibody dose for flow cytometric analysis of intratumoral immune cells (n=4-5 per group). The remainder mice (n=7 per group) were followed for tumor growth (**B**) and survival (**C**). Statistically significant effect of aCD73 on tumor progression was assessed by repeated measure ANOVA in mock-treated mice (0Gy) between day 0 (treatment start) and day 23 and in RT-treated mice (20Gy) between day 0 and day 41. Log-Rank test was used to calculate statistically significant effect of aCD73 on mouse survival for mice treated with the same RT treatment. The experiment was performed twice with similar results. (**D**) Surface expression of

CD73 on TSA cells transduced with doxycycline-inducible shRNA targeting CD73 (TSA^{shCD73}) or a non-silencing sequence (TSA^{shNS}) 3 days following treatment with doxycycline (+DOX) or without doxycycline (-DOX). (**E**) Experimental schema; $1x10^5$ TSA^{shNS} or TSA^{shCD73} cells were subcutaneously (s.c.) injected in the right flank of BALB/c mice on day 0. Doxycycline was fed to the mice starting on day 6 until day 30. Mice were treated with anti-CD73 (aCD73) or isotype control (iso ctrl) antibody on day 10, 13, 16 and 19. Focal RT was delivered to the tumor in a single dose of 20Gy on day 11. (**F**) Tumor growth over time (n=6-9 mice per group). Statistically significant differences in tumor progression between groups was assessed by repeated measure ANOVA in mock-treated mice (0Gy) between day 10 (treatment start) and day 23 and in RT-treated mice (20Gy) between day 10 and day 41. (**G**) Survival in mice bearing TSA^{shNS} or TSA^{shCD73} tumors. Log-Rank (Mantel-Cox) test was used to calculate statistically significant differences in mouse survival between groups. *<0.05, **<0.01, ***<0.001, ****<0.0001.

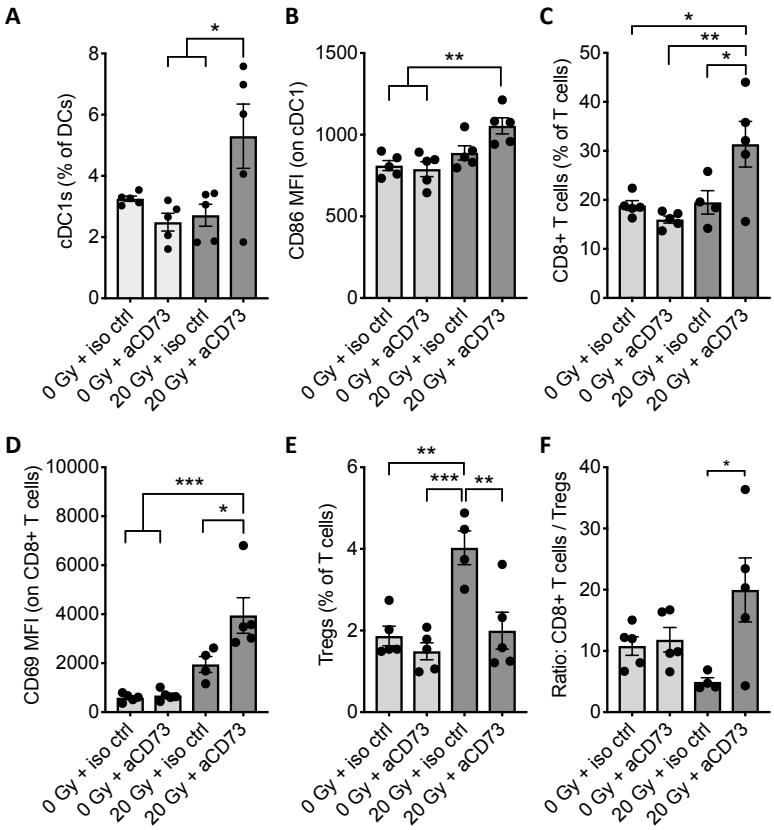

Figure 3. (**A**) Frequency of cDC1 (determined by CD8α+ expression) among DCs. (**B**) Mean fluorescence intensity (MFI) of CD86 by DCs. (**C**) Percentage of CD8+ T cells among T cells. (**D**) MFI of CD69 on CD8+ T cells. (**E**) Percentage of Tregs among T cells. (**F**) Ratio of CD8+ T cell to Tregs. Experiment was

repeated 2-3 times with similar results. Statistically significant changes in immune cell infiltration and MFI was assessed by ANOVA followed by pairwise comparisons using Tukey's method. *p<0.05, **p<0.01, ****p<0.0001, All data shows mean ± s.e.m.

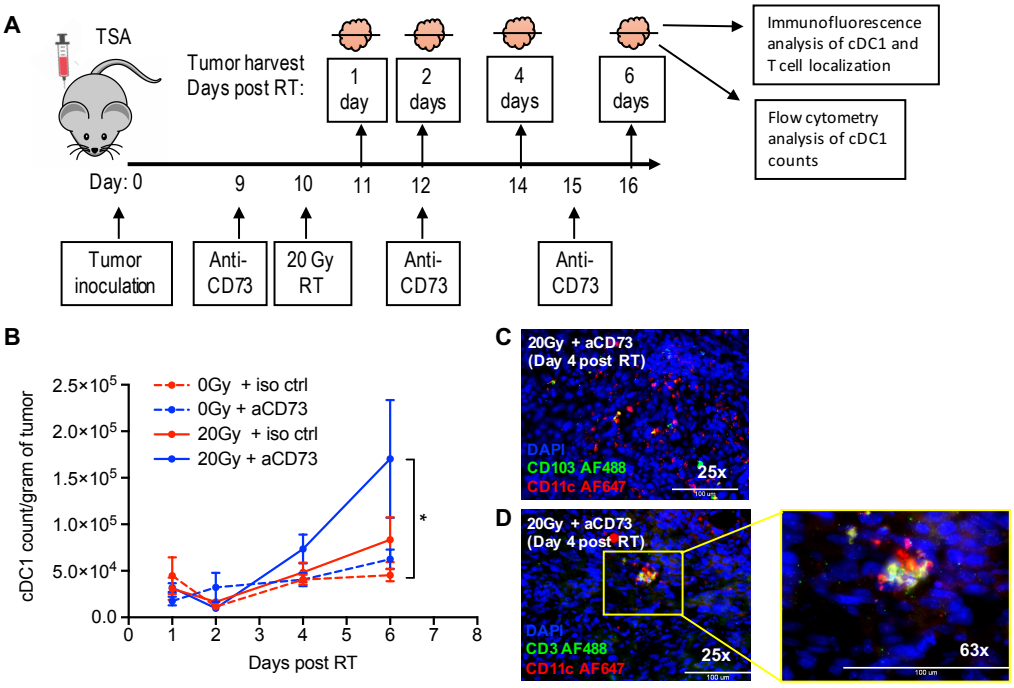

Figure 4. (**A**) Experimental schema. BALB/c mice were inoculated with TSA cells in the right flank on day 0 and treated as indicated. ADO-blockade by anti-CD73 antibody (aCD73, Clone: TY/23) was given at 100 ug, i.p.. Tumors were harvested on day 1, 2, 4 and 6 post-RT. Half of the tumor was used to prepare a single cell suspension and analyzed by flow cytometry for the number of cDC1 using counting beads. The other half of the tumor was used to prepare tissue sections for immunofluorescent staining. (**B**) Number of cDC1 per gram of tumor at various times after treatment with 20 Gy RT (20Gy) or mock-RT treatment (0Gy). ANOVA was used to compare changes in cDC1 density across treatment groups followed by pairwise comparisons using Tukey's method. *p<0.05. All data shows mean±s.e.m. (**C-D**) Representative pictures of multicolor immunofluorescence staining of tumors harvested 4 days post RT. Blue, DAPI staining of tumor cell nuclei. (**C**) Tumor localization of cDC1 identified by expression of CD11c (Alexa Fluor 647) and CD103 (Alexa Fluor 488). CD11c+CD103+ cDC1s are identified by the yellow signal observed when the two channels co-localize. (**D**) Cluster

containing T cells (CD3 Alexa Fluor 488) and DCs (CD11c Alexa Fluor 647) in close contact. Magnification as indicated, bar=100 μm.

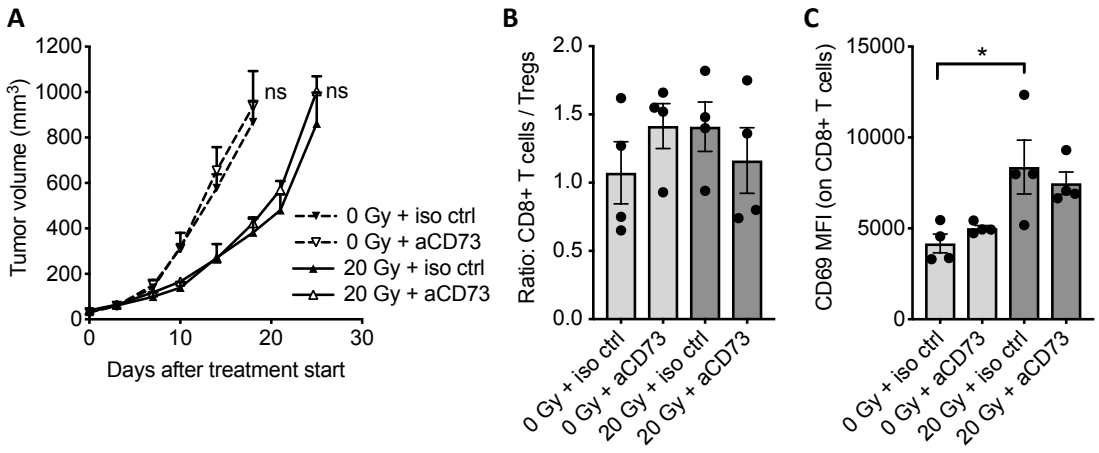

Figure 5. Batf3$^{-/-}$ mice were inoculated subcutaneously with TSA cells and treated with 20Gy RT and anti-CD73 antibody (aCD73, Clone: TY/23, 100μg i.p.) or isotype control (iso ctrl, Clone: 2A3,100 ug, i.p.) as in figure 3A. Mice (n=5 per group) were followed for tumor growth (**A**). Some mice were sacrificed one day after the third antibody dose for flow cytometric analysis of intratumoral immune cells (n=4) (**B, C**). Ratio of CD8/Tregs cells (**B**) and mean fluorescence intensity (MFI) of CD69 on CD8+ T cells (**C**). Statistically significant effect of aCD73 on tumor progression was assessed by repeated measure ANOVA in mock-treated mice (0Gy) between day 0 (treatment start) and day 18 and in RT-treated mice (20Gy) between day 0 and day 25. Statistically significant changes in immune cell infiltration was assessed by ANOVA followed by pairwise comparisons using Tukey's method.

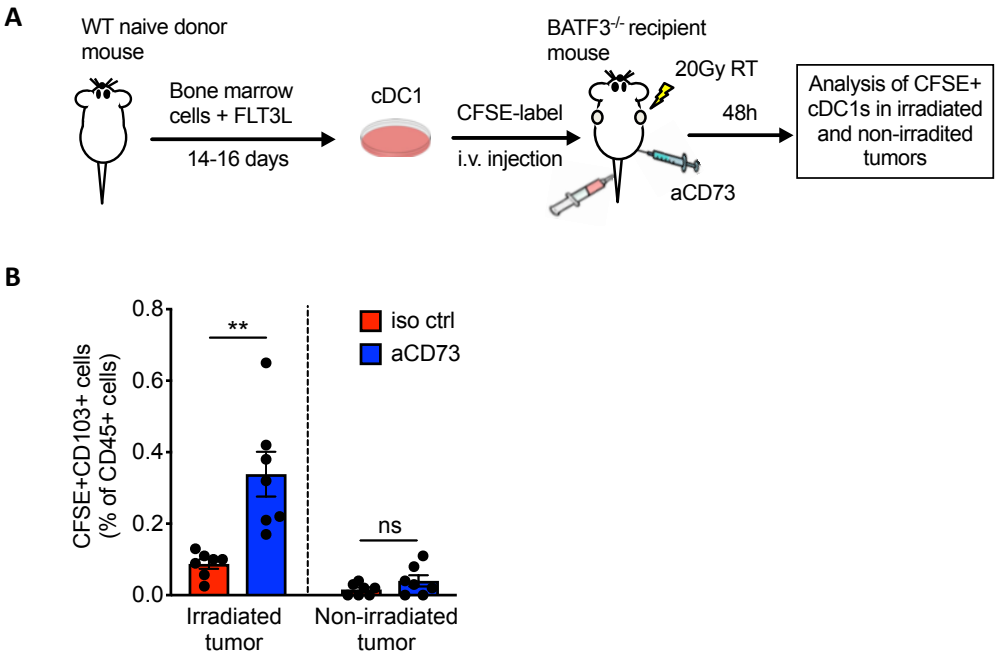

Figure 6. (**A**) Experimental schema for the cDC1 adoptive transfer. Bone-marrow cells were isolated from wild type (WT) mice and cultured with FLT3L and GM-CSF to generate CD103+ cDC1s. BM-derived cDC1s were labeled with CFSE before i.v. injections into Batf3-deficient (Batf3-/-) mice bearing two TSA tumors, 6 hours after irradiation of one tumor with 20Gy and anti-CD73 or iso ctrl mAb administration. Irradiated and non-irradiated tumors were harvested 48 hours after adoptive transfer for analysis by flow cytometry. (**B**) Frequency of CFSE+CD103+ cDC1s among total viable leukocytes in irradiated tumors and non-irradiated tumors (n=7 per group), Welch's T-test (F). *p<0.01, **p<0.01, All data shows mean ± s.e.m.

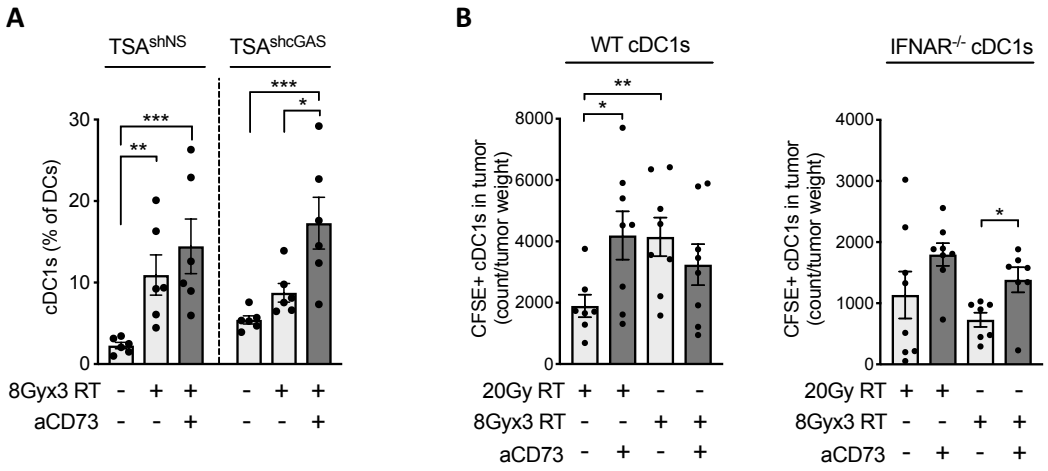

Figure 7. (**A**) WT BALB/c mice were inoculated with primary TSA^{shNS} or TSA^{shcGAS} tumors and treated as above with RT and ADO-blockade by anti-CD73 antibody (aCD73, Clone: TY/23). Tumors were harvested 5 days after last dose of RT for analysis of percentage of cDC1 (determined by expression of XCR1 and CD8a) among total DCs (n=6 per group). ANOVA was used to determine statistically significant difference in DC-infiltration. Experiment was performed twice with similar results. (**B**) cDC1s were prepared from the bone marrow of WT or $Ifnar^{-/-}$ mice as in figure 6A, labeled with CSFE and adoptively transferred into WT BALB/c mice bearing TSA tumors 6 hours after irradiation with 20GyX1 or 8GyX3 and/or anti-CD73 mAb administration. Tumors harvested 48 hours after adoptive transfer and analyzed by flow cytometry for presence of CFSE-labeled cDC1 cells. Bar graphs show the number of CFSE+CD11c+ cells normalized to tumor weight in mice receiving WT cDC1s (left panel) and $Ifnar^{-/-}$ cDC1s (right panel) (n=7-8). Welch's T-test was used to determine statistically significant changes between groups. Data were square root transformed prior to statistical testing. *p<0.05, **p<0.01, ***p<0.001. All data shows mean ± s.e.m.

Milestone (month 24):
Confirmed synergy between RT and ADO-blockade in inducing intratumoral recruitment of DCs and achieving anti-tumor effect

Status: Completed. We show that ADO-blockade (by CD73-blockade or tumor knockdown of CD73 expression) potentiates the ability of RT to control tumor growth. Further we demonstrate that ADO-blockade in combination with RT increases the frequency and density of intratumoral cDC1s and improves CD8 T cell infiltration. We also demonstrate by fluorescence tissue microscopy that cDC1 cells infiltrate tumor tissue following treatment with RT and ADO-blockade. Moreover, we show that ADO-blockade promotes tumor infiltration of adoptively transferred cDC1s in irradiated tumors in a manner independently of IFN type I signaling.

Specific Aim 2:
Determine if ADO blockade in combination with RT enhances the anti-tumor effect of immune checkpoint inhibitors in breast cancer

Major Goal 1 (Months 18-30): Evaluate the immunogenic and anti-tumor effect of RT + ADO-blockade in combination with anti-CTLA-4 treatment

Major activities:

We sought to assess whether ADO-blockade can potentiate the immunogenicity of 20Gy RT and induce systemic anti-tumor effects in combination with anti-CTLA-4 in the 4T1 model. 4T1 is a poorly immunogenic model of TNBC resistant to ICB that rapidly seeds spontaneous metastases to the lungs, which are present by the time the primary tumor is palpable. 4T1 cells do not show a significant RT-induced IFN-I production and priming of anti-tumor CD8 T cells when treated with single 20Gy RT (Demaria S et al. Clin Cancer Res 2005). Since expression of CD73, as well as CD38 and CD203a, was upregulated on 4T1 cells by RT (Figure 1D, right panel), we tested if ADO-blockade by anti-CD73 antibody therapy could improve the local and systemic response of mice bearing 4T1 tumors treated with 20Gy RT. Progression of primary irradiated tumors was monitored (Figure 8A) and mice were sacrificed on day 19 after tumor inoculation for assessment of lung metastasis burden (Figure 8B).

Using the TSA^{shcGAS} tumor model, which upon irradiation with 8Gyx3 is unable to synergize with anti-CTLA-4 and induce systemic anti-tumor immune responses, we assessed whether ADO-blockade could improve this synergy and prolong mouse survival. To this end, we inoculated mice with TSA^{shcGAS} or TSA^{shNS} subcutaneous tumors in the right flank of WT mice (primary tumor) followed by injection of TSA^{shNS} tumors in the contralateral flank (abscopal tumor). Primary tumors were irradiated with 8GyX3 RT, and mice received anti-CD73 and/or anti-CTLA-4 antibodies. Primary and abscopal tumors were measured twice weekly and mice were followed for survival (Experiment layout in Figure 9A).

Specific objectives:

a. Determine whether ADO-blockade can induce synergy between 20Gy RT and anti-CTLA-4 treatment to induce systemic immunity and reduce metastasis in the 4T1 tumor model.

b. Assess the ability of ADO-blockade to restore the abscopal effect of 8Gyx3 RT and anti-CTLA-4 in targeting cGAS-deficient TSA tumors and prolong survival.

Significant results:

a. ADO-blockade by anti-CD73 antibody treatment, beginning when tumors were palpable, did not have any effect on the primary tumor or lung metastases (Figure 8 A-B). When used with 20Gy RT, CD73-blockade enhanced the control of the irradiated tumor but not of lung metastases, suggesting that the immune response elicited by 20Gy+CD73-blockade was not systemically effective. Therefore, we tested whether addition of CTLA-4 blockade could improve the control of the non-irradiated metastases in the lungs of mice treated with 20Gy+CD73-blockade. The double blockade of CD73 and CTLA-4 had no effect without RT, but resulted in a significant decrease in lung metastases when combined with 20Gy RT (Figure 8B). These results confirm the benefits of blocking adenosine generation to improve responses to RT. In addition, they show that ADO-blockade fosters the induction of systemically effective anti-tumor immune responses in mice treated with an RT dose that is otherwise unable to induce abscopal effects in combination with anti-CTLA-4.

b. In line with our hypothesis and previous results, mice bearing primary TSA^{shNS} tumors experienced abscopal responses and prolonged survival following combined 8Gyx3 RT and anti-CTLA-4 compared to mice treated with RT alone, while the synergistic effect of 8Gyx3 RT and anti-CTLA-4 was lost in mice bearing primary TSA^{shcGAS} tumors (Figure 9 B-C). However, ADO-blockade by anti-CD73 antibody treatment, in combination with 8Gyx3 RT and anti-CTLA-4 restored the ability of mice bearing TSA^{shcGAS} tumors experience abscopal responses and prolonged survival (Figure 9 B-C). These data indicate that ADO-blockade is insufficient to induce abscopal responses in combination with RT, but can complement the defective activation of IFN-I by RT in tumors with downregulated cGAS expression.

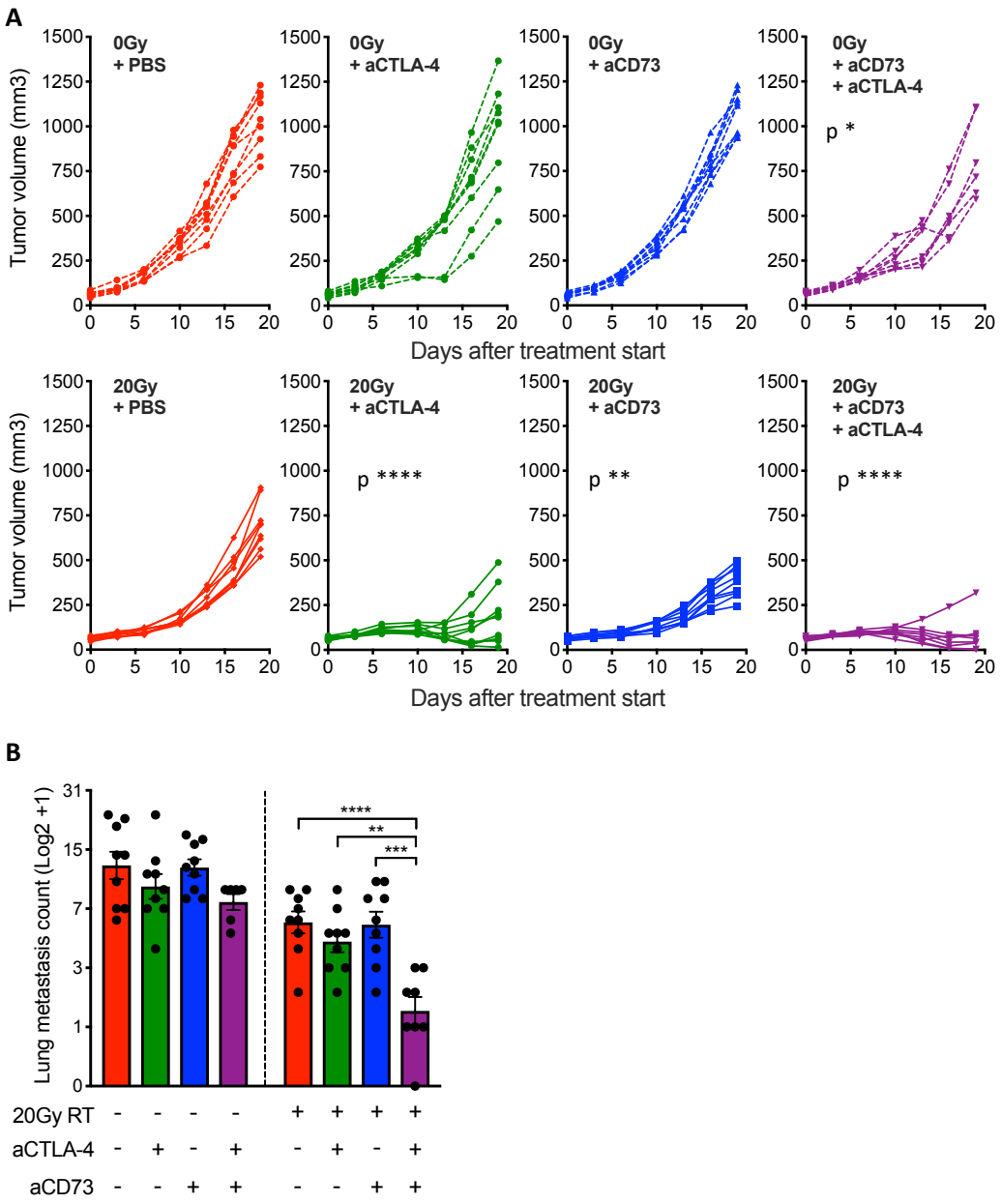

Figure 8. BALB/c mice were inoculated subcutaneously with 4T1 cells in the right flank. Treatment with anti-CD73 mAb (aCD73, Clone: TY/23, 100 µg, i.p.) was started when average tumor volumes approached 40-60 mm3 (day 0) and repeated on day 3, 6 and 9. RT was given as a single dose of 20Gy locally to the tumor on day 1. Anti-CTLA-4 mAb (aCTLA-4, Clone:9H10, 200 ug, i.p.) was administered on day 1, 4 and 7. Mice were followed for tumor growth and euthanized on day 19 for assessment of lung metastases and tumor volume (**A-B**). (**A**) Tumor progression in individual mice. Statistically significant differences in tumor progression between treatment groups was assessed by repeated measure ANOVA. Asterisks indicate P values for the comparison of each treatment group

versus PBS-treated controls for mice treated with the same RT treatment. (**B**) Number of lung metastasis on day 19 after treatment start (n=6-9 per group). Metastases counts were Log2 transformed and ANOVA was used to determine statistically significant differences between treatment groups followed by pairwise comparisons using Tukey's method. *p<0.05, **p<0.01, ***p<0.001, ****p<0.0001. All data shows mean ± s.e.m.

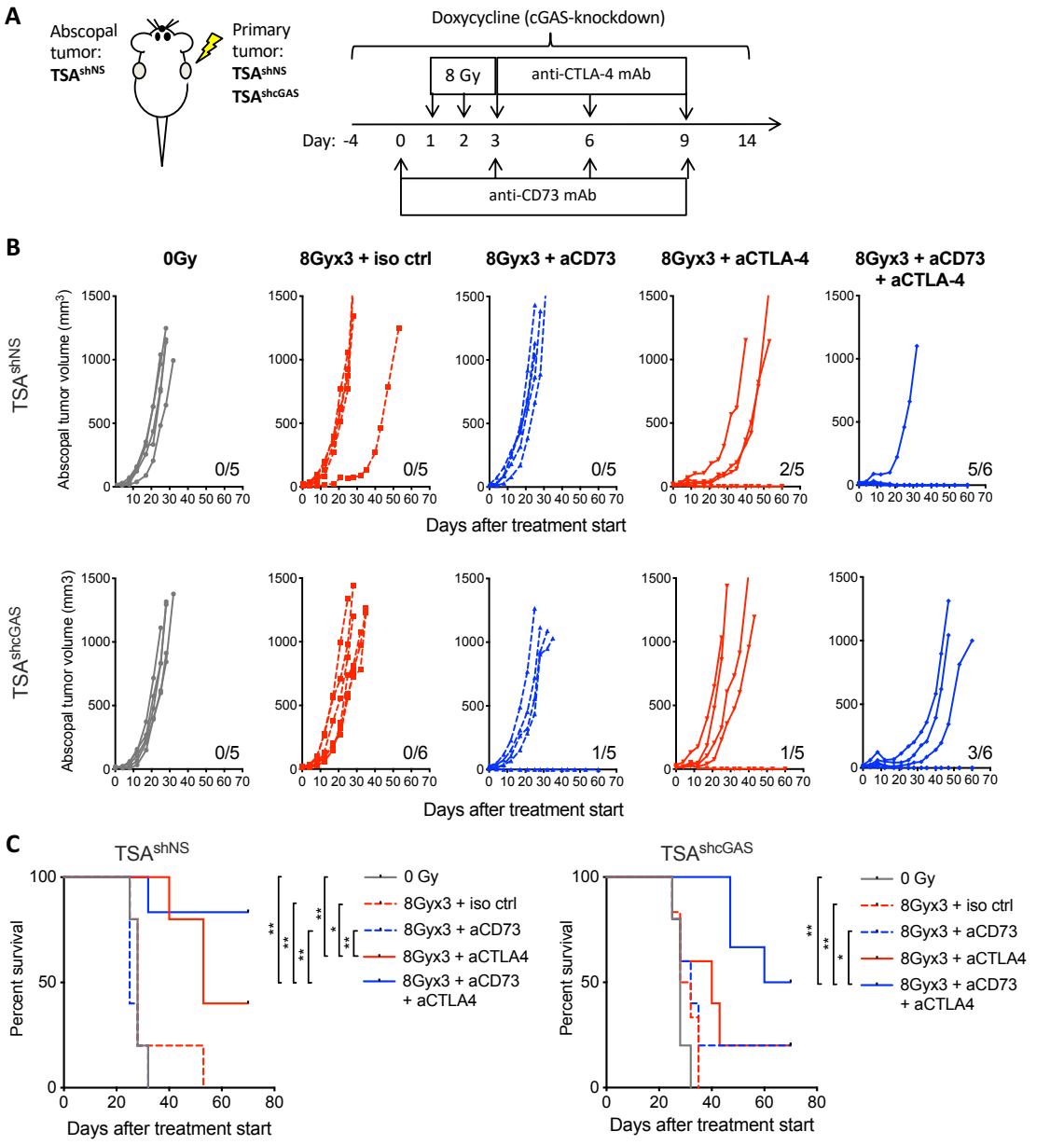

Figure 9. (**A**) Experimental schema. TSA cells expressing a doxycyclin-inducible short hairpin RNA (shRNA) directed against cGAS (TSA^{shcGAS}) or a non-silencing sequence (TSA^{shNS}) were injected in the right flank of WT BALB/c mice (primary tumors). Two days later TSA^{shNS} was injected in the contralateral flank (abscopal tumors). Doxycyclin was fed to mice once the tumors became palpable (day -4) and treatment started when primary tumors reached a volume of 40-60 mm3 (day 0). RT was given in 3 daily doses of 8Gy to the primary tumor. ADO-blockade by anti-CD73 mAb (aCD73, Clone: TY/23, 100 μg) and anti-CTLA-4 mAb (aCTLA-4, Clone: 9H10, 200 ug) were administered i.p. as indicated, and mice followed for tumor growth and survival. (**B**) Abscopal tumor growth overtime. Each line represents an individual mouse (n=5-6). Numbers indicate the number of mice with complete tumor regression over the total in each group. (**C**) Survival in mice bearing primary TSA^{shNS} tumors or TSA^{shcGAS} tumors. Log-Rank (Mantel-Cox) test was used to calculate statistically significant differences in mouse survival between treatment groups.

Major Goal 2 (Months 25-36): Evaluate the immunogenic and anti-tumor effect of RT + ADO-blockade in combination with anti-PD-1 treatment

Major activities:
As the project has developed we have gained increased understanding of the biology of RT-induced induction of adenosinergic signaling, and this has informed our choice of models to test combinations with ICB. Since we have found recruitment and activation of cDC1 to be important for the synergistic effect of RT and ADO-blockade, we decided to focus our ICB combination studies on anti-CTLA-4 which acts primarily on the priming phase of the RT-induced immune response where the actions of cDC1 cells are crucial, rather than anti-PD-1 which acts on the effector phase of the immune response.

Milestone (month 36):
Induction of protective anti-tumor immunity by in situ tumor vaccination following combined treatment with RT + ADO-blockade + ICB

Status: Completed. We have confirmed that ADO-blockade can potentiate the ability of RT and ICB to induce in situ tumor vaccination and trigger systemic immune responses two tumor models where IFN type I signaling is hampered. In the 4T1 model, we showed that ADO-blockade could potentiate the effect of 20Gy RT and anti-CTLA-4 to reduce tumor metastasis. Further, we show that ADO-blockade can restore the ability of 8Gyx3 RT and anti-CTLA-4 to trigger abscopal effects independently of cGAS/STING signaling.

What opportunities for training and professional development has the project provided?

During the reporting period, I have attended department lab meetings where I have presented data from the project bi-monthly. Moreover, I have presented findings from the project at the following international conferences:

- 5th Annual Immuno-Oncology Young Investigators' Forum, Houston, Texas, USA, April 27, 2019.

- 5th CRI-CIMT-EATI-AACR International Cancer Immunotherapy Conference (CICON 2019), Paris, France, September 25 - 28, 2019.

How were the results disseminated to communities of interest?

Nothing to report

What do you plan to do during the next reporting period to accomplish the goals?

Nothing to report

4. IMPACT

What was the impact on the development of the principal discipline(s) of the project?

Our findings showing that ADO-blockade by anti-CD73 antibody treatment can potentiate the radiation-induced immune response against poorly immunogenic mammary tumors, could have important implications for the development of novel treatment strategies for breast cancer patients. Antibodies targeting CD73 are currently being tested in clinical trials and our finding that anti-CD73 antibody treatment can increase the synergy of RT and ICB independently of IFN type I signaling via cGAS/STING could have an impact for breast cancer patients. Particularly to those patients that are refractory

to ICB or have tumors with deficient cGAS/STING signaling (Konno H, Oncogene 2018), thus increasing the number of patients that could respond to ICB therapy.

What was the impact on other disciplines?

Nothing to report

What was the impact on technology transfer?

Nothing to report

What was the impact on society beyond science and technology?

Nothing to report

5. CHANGES/PROBLEMS

Nothing to report

6. PRODUCTS

Publications, conference papers, and presentations

Journal publications:

CD73-blockade promotes IFN type I-independent Batf3-dendritic cell infiltration of irradiated tumors and tumor rejection. Wennerberg E, Spada S, Rudqvist NP, Lhuillier C, Gruber S, Chen Q, Zhang F, Zhou X, Gross SS, Formenti SC, Demaria S. *Cancer Immunol Res*. 2020 Apr;8(4):465-478. doi: 10.1158/2326-6066.CIR-19-0449. Epub 2020 Feb 11.

Article attached in appendices (Appendix #1)

Books or other non-periodical, one-time publications:

Nothing to report

Other publications, conference papers, and presentations:

1. Oral abstract presentation: **Adenosine generation in irradiated tumors represents a barrier to radiation-induced anti-tumor immunity.**
   Presented at: 5th Annual Immuno-Oncology Young Investigators' Forum (IOYIF), Houston, Texas, USA, April 27, 2019.

   Abstract attached in appendices (Appendix #2)

2. Poster presentation: **CD73 blockade potentiates radiation-induced tumor infiltration of conventional type I dendritic cells and abscopal anti-tumor effects in combination with immune checkpoint blockade.**
   Presented at: 5th CRI-CIMT-EATI-AACR International Cancer Immunotherapy Conference (CICON), Paris, France, September 25 - 28, 2019.

   Abstract attached in appendices (Appendix #3)

Website(s) or other Internet site(s)

Nothing to report

Technologies or techniques

Nothing to report

Inventions, patent applications, and/or licenses

Nothing to report

Other Products

Nothing to report

7. PARTICIPANTS & OTHER COLLABORATING ORGANISZATIONS

What individuals have worked on the project?

Name:	*Erik Wennerberg*
Project Role:	*PI*
Researcher Identifier (e.g. ORCID ID):	https://orcid.org/0000-0001-7689-5988
Nearest person month worked:	12
Contribution to Project:	*Dr. Wennerberg has planned and analyzed all experiments and has performed experimental work*
Funding Support:	N/A

Has there been a change in the active other support of the PD/PI(s) or senior/key personnel since the last reporting period?

Nothing to report

What other organizations were involved as partners?

Nothing to report

8. SPECIAL REPORTING REQUIREMENTS

Nothing to report

9. APPENDICES

1. Journal publication: **CD73-blockade promotes IFN type I-independent Batf3-dendritic cell infiltration of irradiated tumors and tumor rejection.** Wennerberg E, Spada S, Rudqvist NP, Lhuillier C, Gruber S, Chen Q, Zhang F, Zhou X, Gross SS, Formenti SC, Demaria S. *Cancer Immunol Res*. 2020

2. Meeting abstract: **Adenosine generation in irradiated tumors represents a barrier to radiation-induced anti-tumor immunity**
   Presented at: 5th Annual Immuno-Oncology Young Investigators' Forum (IOYIF), Houston, Texas, USA, April 27, 2019. Abstract was selected for oral presentation.

3. Meeting abstract: **CD73 blockade potentiates radiation-induced tumor infiltration of conventional type I dendritic cells and abscopal anti-tumor effects in combination with immune checkpoint blockade.**
   Presented at: 5th CRI-CIMT-EATI-AACR International Cancer Immunotherapy Conference (CICON), Paris, France, September 25 - 28, 2019. Abstract was selected for poster presentation.

Published OnlineFirst February 11, 2020; DOI: 10.1158/2326-6066.CIR-19-0449

CD73 Blockade Promotes Dendritic Cell Infiltration of Irradiated Tumors and Tumor Rejection

Erik Wennerberg[1], Sheila Spada[1], Nils-Petter Rudqvist[1], Claire Lhuillier[1], Sylvia Gruber[1], Qiuying Chen[2], Fengli Zhang[2], Xi K. Zhou[3], Steven S. Gross[2], Silvia C. Formenti[1], and Sandra Demaria[1,4]

ABSTRACT

The ability of focal radiotherapy to promote priming of tumor-specific CD8$^+$ T cells and increase responses to immunotherapy is dependent on infiltration of the tumor by Batf3-dependent conventional dendritic cell type 1 (cDC1) cells. Such infiltration is driven by radiotherapy-induced IFN type I (IFN-I). Other signals may also modulate cDC1 infiltration of irradiated tumors. Here we found increased expression of adenosine-generating enzymes CD38 and CD73 in irradiated mouse and human breast cancer cells and increased adenosine in mouse tumors following radiotherapy. CD73 blockade alone had no effect. CD73 blockade with radiotherapy restored radiotherapy-induced cDC1 infiltration of tumors in settings where radiotherapy induction of IFN-I was suboptimal. In the absence of radiotherapy-induced IFN-I, blockade of CD73 was required for rejection of the irradiated tumor and for systemic tumor control (abscopal effect) in the context of cytotoxic T-lymphocyte–associated protein 4 blockade. These results suggest that CD73 may be a radiation-induced checkpoint, and that CD73 blockade in combination with radiotherapy and immune checkpoint blockade might improve patient response to therapy.

Introduction

In patients with preexisting antitumor immunity, immune checkpoint blockade (ICB) therapy with antibodies targeting cytotoxic T-lymphocyte–associated protein 4 (CTLA-4) and programmed cell death 1 (PD-1) or its ligand PD-L1 has shown clinical efficacy. Such therapy unleashes the effector function of tumor-specific CD8$^+$ T cells (1). However, ICB therapy is ineffective for most patients, prompting the search for strategies that work in concert with ICB to immunize the patients against their tumor (2). Focal radiotherapy can elicit antitumor T-cell responses in combination with ICB in multiple ICB-resistant mouse tumor models (reviewed in ref. 3). The combination of radiotherapy and ICB is also being tested in the clinic (4). Success is variable (5, 6), emphasizing the need to optimize the use of radiotherapy to generate antitumor T-cell responses and enhance responses to ICB therapy (7).

Mechanistic studies have revealed a role of the IFN type I (IFN-I) pathway in radiotherapy immunogenicity (8–10). In poorly immunogenic tumors, cancer cell–intrinsic IFN-I production promotes tumor infiltration by conventional dendritic cells type 1 (cDC1), a subset of dendritic cells (DC) whose ontogeny is dependent on the transcription factor basic leucine zipper transcription factor ATF-like (Batf3; ref. 9). cDC1s, which cross-present tumor antigens to CD8$^+$ T cells, are essential for antitumor immune responses (11). Radiotherapy-induced T-cell priming was abrogated in Batf3-deficient (Batf3$^{-/-}$) mice (9). IFN-I was implicated in the synergistic and abscopal response of patients with metastatic lung cancer who were treated with both ipilimumab and radiotherapy (6). Induction of IFN-I by radiotherapy is mediated via the cyclic GMP-AMP synthase (cGAS) through the stimulation of interferon genes (STING) pathway, which is frequently downregulated in tumors (9, 10, 12). Here, we search for alternative pathways to promote radiotherapy-induced cDC1 infiltration.

The proinflammatory molecule ATP is released from cells undergoing radiation-induced cell death (13), and promotes the recruitment and activation of DCs (14, 15). Extracellular ATP concentrations are tightly regulated by ectoenzymes, which are often overexpressed in tumors (16). Following hydrolysis of ATP into ADP and AMP by the ectonucleotidase CD39, AMP is irreversibly dephosphorylated into adenosine by CD73. Adenosine can also be generated by conversion of NAD$^+$ into ADP-ribose and AMP by CD38 and CD203a (17, 18).

Adenosine elicits multiple anti-inflammatory and immunosuppressive effects, mediated by the adenosine receptors A1, A2A, A2B, and A3 expressed on immune cells (19). These effects include promoting a tolerogenic phenotype in DCs with reduced ability to induce Th1 polarization of naïve T cells (20), inducing T-cell anergy and promoting regulatory T cell (Treg) differentiation (21). Elevated expression of CD73 is associated with a poor prognosis in triple-negative breast cancer (TNBC) and other tumor types (22–24). Elevated tumor expression of CD38 has been observed in melanoma (17) and is implicated in acquired resistance to anti-PD-1 therapy (25). The therapeutic potential of blocking adenosine pathways with mAbs targeting CD73 and small-molecule inhibitors of A2AR is being tested in phase I trials in patients with solid tumors (16, 26).

Here, we investigated how adenosine regulates radiation-induced immune responses. We found that expression of CD73 and ectonucleotidases was upregulated by radiation in human and mouse breast cancer cells. Adenosine content was increased in irradiated tumors. CD73 blockade enhanced (i) tumor infiltration by cDC1s in the absence of radiation-induced IFN-I, (ii) response of the

[1]Department of Radiation Oncology, Weill Cornell Medicine, New York, New York. [2]Department of Pharmacology, Weill Cornell Medicine, New York, New York. [3]Division of Biostatistics and Epidemiology, Department of Healthcare Policy and Research, Weill Cornell Medicine, New York, New York. [4]Department of Pathology and Laboratory Medicine, Weill Cornell Medicine, New York, New York.

Note: Supplementary data for this article are available at Cancer Immunology Research Online (http://cancerimmunolres.aacrjournals.org/).

Current address for S. Gruber: Department of Radiation Oncology, Medical University of Vienna, Vienna, Austria.

Corresponding Author: Sandra Demaria, Weill Cornell Medicine, 1300 York Avenue, Box 169, New York, NY 10065. Phone: 646-962-2092; E-mail: szd3005@med.cornell.edu

Cancer Immunol Res 2020;8:465–78

doi: 10.1158/2326-6066.CIR-19-0449

Published OnlineFirst February 11, 2020; DOI: 10.1158/2326-6066.CIR-19-0449

irradiated tumor, and (iii) induction of systemic antitumor T-cell responses.

Materials and Methods

Tumor cells and reagents

BALB/c-derived mammary carcinoma cell lines TSA and 4T1 were obtained from Dr. Lollini (Alma Mater Studiorum University of Bologna, Bologna, Italy) and Dr. Miller (Michigan Cancer Foundation, Detroit, MI), respectively (27, 28) in 2002, and authenticated by IDEXX Bioresearch in 2019. Human TNBC cells MDA-MB-231 and 4175TR were purchased from ATCC and obtained from Dr. Massague (Memorial Sloan Kettering Cancer Center, New York, NY), respectively, and were authenticated in 2016 by IDEXX Bioresearch. Cells were screened for *Mycoplasma* using the Lookout Mycoplasma Detection Kit (Sigma) prior to preparation of working stocks of frozen cells, and thawn 3 to 5 days before use in all experiments. Tumor cells were grown in DMEM (Gibco) cell culture medium supplemented with 10% FBS, 2 mol/L L-glutamine, 100 U/mL penicillin, 100 μg/mL streptomycin, and 2.5×10^{-5} mol/L β-mercaptoethanol (Life Technologies; complete medium). Rat mAb to mouse CD73 (TY/23, BE0209), rat IgG2a isotype control (2A3, BE0089), and hamster mAb to mouse CTLA-4 (9H10, BE0131) were purchased from BioXCell.

Animals

Wild-type (WT) BALB/c female mice were purchased from Taconic Biosciences. BALB/c interferon-α/β-receptor-1–deficient ($Ifnar1^{-/-}$) mice were provided from Dr. Durbin (Rutgers University, NJ). BALB/c $Batf3^{-/-}$ mice were purchased from Jackson Laboratories and bred in-house. All mice were maintained under pathogen-free conditions in the animal facility at Weill Cornell Medicine (New York, NY) or New York University School of Medicine (New York, NY). All mouse experiments were approved by the Institutional Animal Care and Use Committee of each institution.

Generation of tumor cells with cGAS and CD73 knockdown

TSA cells expressing a tetracycline-inducible short-hairpin RNA (shRNA)-targeting cGAS (TSA^{shcGAS}) or a nonsilencing construct (TSA^{shNS}) have been described previously (9). shRNA construct targeting CD73 (TSA^{shCD73}) were prepared using a similar protocol. Briefly, HEK293-FT cells were transfected with the packaging plasmids pPAX2 and pMD2 and a pTRIPZ vector containing a tetracycline-inducible promoter driving the expression of a TurboRFP fluorescent reporter (GE Dharmacon Technology). shRNA directed against CD73 mRNA (*Nt5e*, mouse-shRNA: AAGCATGACTCTGGTGATCAAG) was cloned into pTRIPZ using *Eco*RI and *Xho*I restriction sites. TSA cells were transduced with cell-free virus-containing supernatants and selected with 4 μg/mL of puromycin during 48 hours.

Mouse tumor challenge and treatment

BALB/c mice were inoculated with 1×10^5 TSA, TSA^{shCD73}, TSA^{shcGAS}, TSA^{shNS}, or with 5×10^4 4T1 cells, respectively, by subcutaneous injection in the right flank (primary tumor). In some experiments, BALB/c mice were injected subcutaneously in the contralateral flank with TSA or TSA^{shNS} cells (abscopal tumor) 2 days following primary tumor inoculation. When applicable, cGAS or CD73 knockdown was induced by administration of doxycycline (100 μg/mL) in drinking water *ad libitum* starting 4 days prior to treatment start, which was replenished every 4 days until day 28 and 30, respectively. Mice were randomized to treatment groups when primary tumors reached an average tumor volume of 40–60 mm^3 and abscopal tumors reached an average tumor volume of 15–20 mm^3. All mice (including mock-irradiated mice) were anesthetized by intraperitoneal injection of Avertin (240 mg/kg). Using the Small Animal Radiation Research Platform (Xstrahl), radiotherapy was delivered at 271 cGy/minute directed to the primary tumor as a single dose of 8, 12, or 20 Gy or with three fractions of 8 Gy delivered on consecutive days (8 Gy × 3). Anti-CD73 was administered intraperitoneally in four doses of 100 μg 3 days apart starting the day prior to radiotherapy. Anti–CTLA-4 was administered intraperitoneally in three doses of 200 μg 3 days apart starting on the last day of radiotherapy. Tumors were measured by caliper every 2–3 days and volumes calculated using the formula: length × $width^2$ × π/6. Mice were sacrificed when tumor exceeded 1,000 mm^3 or if animals showed signs of distress.

Assessment of lung metastatic burden in 4T1 tumor model

BALB/c mice were sacrificed at day 19 after the start of treatment. Mouse lungs were excised and fixed in 4% paraformaldehyde for 24 hours. Lung sample treatments were blinded to investigators and gross lung metastases were enumerated using a dissection microscope.

Preparation of cells for flow cytometry analysis

Human and murine tumor cells were cultured until 80% confluent. Cells were either mock-irradiated (0 Gy) or treated with 8, 12, 20 Gy, or 8 Gy × 3. The culture medium was replaced with fresh medium after radiotherapy and incubated for 24 hours after which cells were trypsinized and single-cell suspensions were washed in PBS before staining. Mouse flank tumors were excised, weighed, and single-cell suspensions were generated following digestion using a Tumor Dissociation Kit (Miltenyi Biotec, 130-096-730) and the GentleMACS Octo Dissociator (Miltenyi Biotec). Single-cell suspensions from tumors were strained through a 70 μm filter before staining.

Flow cytometry analysis

Cells were stained with fixable viability dye in PBS, 20 minutes, 4°C, then stained for surface markers using fluorochrome-conjugated antibodies (listed in Supplementary Table S1) for 20 minutes, 4°C. Cells were fixed using the Cytofix/Cytoperm Kit (BD Biosciences, 554714) followed by staining for intracellular targets. Samples were acquired on LSRII (BD Biosciences) or MACSQuant (Miltenyi Biotec) flow cytometers and analyzed using FlowJo Software (Tree Star). Tregs were identified as $CD4^+CD25^+FoxP3^+$, DCs were identified as $CD11c^+MHCII^+$ or $CD11c^+$, and cDC1 in the DC population were identified by expression of CD103, XCR1, and/or CD8α. To account for changes in autofluorescence induced by treatment, for each sample the mean fluorescence intensity (MFI) of antibody-stained cells was corrected for the MFI of cells stained with fluorescence minus one as indicated.

Immunostaining of tumor tissue and image acquisition

Subcutaneous mouse tumors were fixed in 4% paraformaldehyde for 24 hours at 4°C, placed in 30% sucrose solution for 24 hours, and frozen in optimal cutting temperature compound (Sakura Finetek). Tissue sections (7 μm) were incubated with PBS containing 50 mmol/L glycine for 15 minutes, followed by permeabilization with PBS containing 0.05% Tween (Sigma) and 0.01% Triton-X (FisherBiotech, Thermo Fisher Scientific). Tumor sections were blocked with PBS containing 1% BSA and 5% goat serum for 1 hour and stained with primary antibodies (listed in Supplementary Table S1) at 4°C overnight. Tumor sections were stained with secondary antibodies (listed

Published OnlineFirst February 11, 2020; DOI: 10.1158/2326-6066.CIR-19-0449

in Supplementary Table S1) for 1 hour and mounted with DAPI-containing mounting medium (Vector Laboratories). Images of tumor sections were acquired using the Axio Observer Inverted Fluorescence microscope (Zeiss).

Adoptive transfer experiments

Bone marrow cells isolated from tibia and femur of WT or Ifnar$^{-/-}$ BALB/c mice were plated in petri dishes (Thermo Fisher Scientific) in RPMI1640 (Gibco) complete medium containing 3% GM-CSF (generated from GM-CSF cell line; ref. 29) and 200 ng/mL FMS-like tyrosine kinase 3 ligand (FLT3L; eBioscience) and 20 ng/mL IL4 (eBioscience) to generate cDC1s (30). On day 14–16 of culture, cells were analyzed by flow cytometry for cDC1 percentage, which was consistently >80%, and labeled with carboxyfluorescein (CFSE; CellTrace CFSE Cell Proliferation Kit, Invitrogen, C34554). Batf3$^{-/-}$ mice or WT mice bearing primary and abscopal TSA tumors (60–70 mm^3) received focal radiotherapy to the primary tumor either as a single dose of 20 Gy or 8 Gy × 3. Two hours prior to the last radiotherapy dose, mice were injected intraperitoneally with anti-CD73 or isotype control mAb. Six hours following the last radiotherapy dose, all mice received intravenous injections of CFSE-labeled cDC1s (1 × 10^6 cells/mouse). After 48 hours, irradiated and nonirradiated tumors were harvested, homogenized into single-cell suspensions as described above, and analyzed by flow cytometry for infiltration of CFSE-labeled cDC1s. Gating strategy is described in Supplementary Fig. S1.

Extraction of tumor metabolites for analysis by LC/MS

Mouse tumors were excised and immediately snap-frozen. Tumor tissues were washed twice with ice-cold PBS, followed by metabolite extraction using −70°C 80% methanol in water (LC/MS grade methanol, Thermo Fisher Scientific). The tissue–methanol mixture was subjected to bead-beating for 45 seconds using a Tissuelyser Cell Disrupter (Qiagen). Extracts were centrifuged for 5 minutes at 5,000 rpm to pellet insoluble material and supernatants were transferred to clean tubes. The extraction procedure was repeated two additional times and all three supernatants were pooled, dried in a Vacufuge (Eppendorf), and stored at −80°C until analysis. The methanol-insoluble protein pellet was solubilized in 0.2 mol/L NaOH at 95°C for 20 minutes and quantified using the Bio-Rad DC Assay (Bio-Rad). On the day of metabolite analysis, dried cell extracts were reconstituted in 70% acetonitrile with 0.2% ammonium hydroxide at a relative protein concentration of 4 μg/mL and 4 μL of the reconstituted extract was injected for LC/MS-based untargeted metabolite profiling.

LC/MS analysis of adenosine in tumors

Metabolomic analysis was performed on tumor extracts by LC/MS as described previously (31), using a platform comprised of an Agilent Model 1290 Infinity II liquid chromatography system coupled to an Agilent 6550 iFunnel time-of-flight MS analyzer. Chromatography of polar metabolites was performed using aqueous normal phase chromatography on a Diamond Hydride Column (MicroSolv). Mobile phases consisted of: (A) 50% isopropanol, containing 0.025% acetic acid, and (B) 90% acetonitrile containing 5 mmol/L ammonium acetate. To eliminate the interference of metal ions on chromatographic peak integrity and electrospray ionization, EDTA was added to the mobile phase at a final concentration of 6 μmol/L. The following gradient was applied: 0–1.0 minutes, 99% B; 1.0–15.0 minutes, to 20% B; 15.0–29.0 minutes, 0% B; and 29.1–37 minutes, 99% B. Raw LC/MS data were extracted by MassHunter Profinder 8.0 and compared with a pure adenosine standard using MassProfiler Professional 14.9 software and a default data normalization method of median baselining and LOG2 transformation (Agilent Technologies).

Soluble CD73 measurement by ELISA

Plasma samples from patients with metastatic breast cancer participating in a prospective randomized trial assessing the efficacy of the anti-TGFβ fresolimumab in combination with radiotherapy (7.5 Gy × 3; NCT01401062; ref. 32) were analyzed for concentration of soluble CD73 (sCD73) by ELISA (Abcam, ab213761). Concentration of sCD73 was measured in samples collected before treatment (baseline) and at week 2, after completion of radiotherapy administered during week one. Supernatants from MDA-MB-231 and 41745TR tumor cells mock-treated or irradiated with 8 Gy × 3 were harvested 24 hours after treatment, and measured for sCD73 by ELISA. sCD73 concentrations were normalized to the viable cell count at the time of supernatant harvest.

Statistical analysis

Differences in mouse tumor volume (log transformed) between treatment groups was evaluated using repeated measures ANOVA from start of treatment until the indicated timepoints. Mouse survival was illustrated using the Kaplan–Meier method and differences in survival between treatment groups were evaluated using the log-rank test. Differences in frequency of intratumoral cell populations and MFI values between treatment groups were calculated using ANOVA and Tukey test was applied for pairwise comparisons between treatment groups. Differences in adenosine abundance and tumor infiltration of adoptively transferred cDC1s between treatment groups were calculated using Welch t test. When appropriate, data were $\log_2$ or square root transformed prior to statistical analysis to ensure the underlying model assumptions were satisfied. Percentage of change in sCD73 plasma concentration was analyzed using a one-sample t test. Statistical analysis was performed using Prism version 8 (GraphPad). All statistical tests performed were two-tailed, and $P < 0.05$ was considered as statistically significant. Except where indicated, all data show mean ± SEM.

Results

Radiation increases ectonucleotidases that generate adenosine in mouse breast tumors

Adenosine is induced in response to tissue damage and inflammation (33), thus we hypothesized that radiation-induced damage to the tumor could lead to an increase in adenosine concentration. To test the effects of radiation on adenosine concentration within the tumor microenvironment, BALB/c mice bearing syngeneic subcutaneous TSA mammary carcinoma were treated with focal radiotherapy and tumors were analyzed 24 hours later. Irradiation did not have a significant effect on adenosine concentrations until treatment with 20 Gy (148% mean increase over untreated control tumors; **Fig. 1A**).

To explore the mechanisms of this adenosine increase, we analyzed tumor expression of the ectonucleotidases CD39 and CD73 in the CD45$^-$ and CD45$^+$ compartment, the latter representing from 23% to 36% of total viable cells, with no statistically significant differences between the groups. At 24 hours after radiotherapy, CD39, which was expressed only by CD45$^+$ cells, did not show significant changes (**Fig. 1B** and **C**). CD73 was expressed by a subset of CD45$^+$ cells and

Published OnlineFirst February 11, 2020; DOI: 10.1158/2326-6066.CIR-19-0449

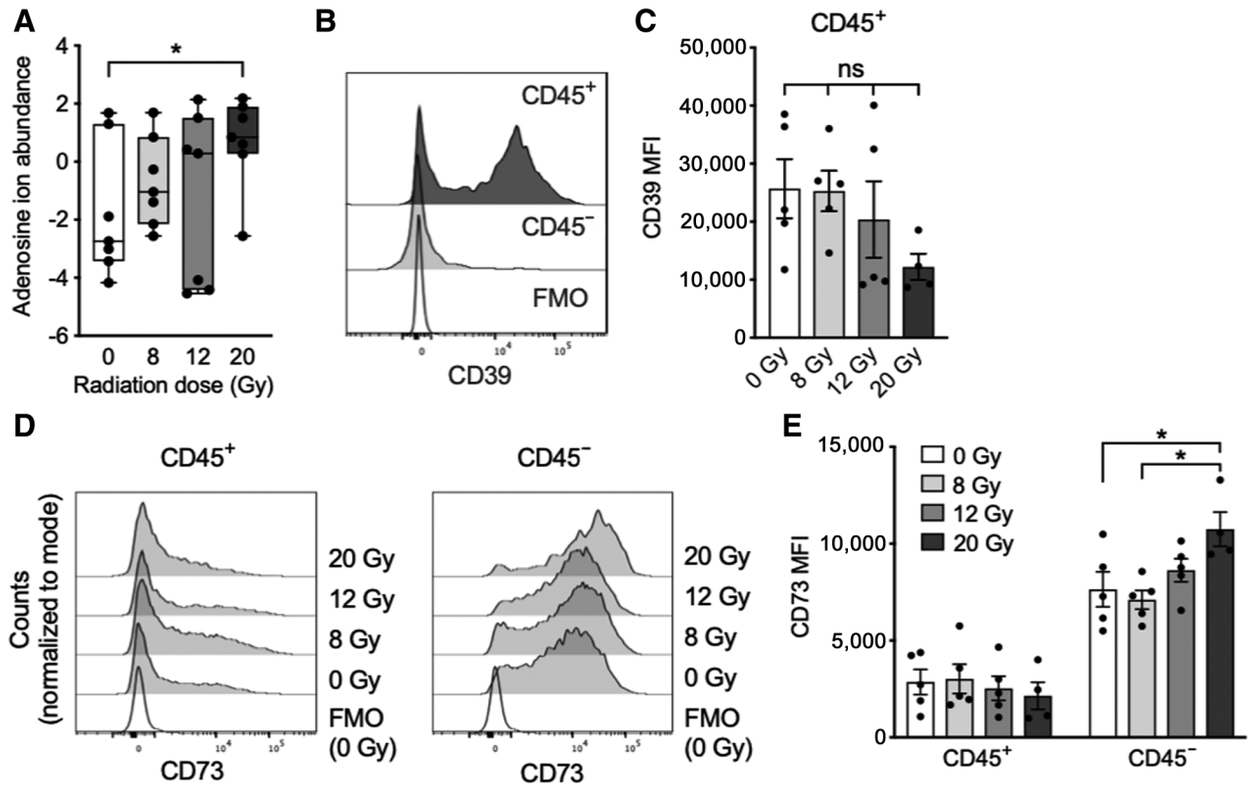

Figure 1.

High-dose radiotherapy induces adenosine increase in mouse tumors. Mice bearing subcutaneous TSA tumors were treated with focal radiotherapy at different doses as indicated. Twenty-four hours after radiotherapy, tumors were harvested for analysis. **A,** Adenosine ion abundance. Data were normalized to median and $\log_2$ transformed. Plot shows median values and interquartile range. $n = 7$ per group, Welch t test, *, $P < 0.05$. The experiment was performed twice with similar results. **B** and **C,** Surface expression of CD39 on CD45$^+$ and CD45$^-$ cells. Representative histograms (**B**) and MFI on CD45$^+$ cells (**C**). **D** and **E,** Surface expression of CD73 on CD45$^+$ and CD45$^-$ cells. Representative histograms (**D**) and MFI (**E**). Flow cytometry data show mean ± SEM. $n = 4$–5 per group, ANOVA followed by Tukey test (ns, nonsignificant; *, $P < 0.05$). FMO, fluorescence minus one.

its expression did not change in irradiated tumors. In contrast, most CD45$^-$ cells expressed abundant CD73 in untreated tumors and increased expression after treatment with 20 Gy radiotherapy (**Fig. 1D** and **E**).

Given the effect of radiotherapy on the expression of CD73 in the CD45$^-$ compartment of TSA tumors *in vivo*, we sought to investigate the effects of radiation on the expression of the ectonucleotidases that generate adenosine *in vitro*. Expression of CD39 was not detectable on TSA or on 4T1 mouse mammary carcinoma cells (Supplementary Fig. S2A), whereas CD73 was expressed and upregulated by radiation. TSA and 4T1 cells also expressed CD38 and CD203a, the two members of the noncanonical adenosine pathway and CD38 was significantly upregulated by radiation in both cell lines (**Fig. 2A–D**). In 4T1 cells, CD203a expression was significantly upregulated after radiation (**Fig. 2C** and **D**). These data show that radiation induces this immunosuppressive pathway.

Radiation increases CD73 expression and release in human breast cancer

To investigate whether human breast cancer cells respond to radiation by upregulating the ectonucleotidases that generate adenosine, we treated the human TNBC cell lines MDA-MB-231 and 4175TR with various radiation doses and analyzed them for expression of CD38 and CD73. Similar to mouse breast cancer cells, both MDA-MB-231 and 4175TR cells were negative for CD39 (Supplementary Fig. S2B) and showed a significant increase in surface expression of CD38 and CD73 at all radiation doses tested. The largest increase in expression of CD38 was seen after 8 Gy × 3 radiotherapy (**Fig. 3A**; Supplementary Fig. S3).

CD73 is shed following substrate binding and is detectable in the circulation. sCD73 amounts are associated with poor prognosis in patients with melanoma, suggesting that circulating sCD73 reflects an immunosuppressive tumor microenvironment (34, 35). To test whether the increased cell surface expression of CD73 induced by radiation on human breast cancer cells is associated with an increase in shedding, sCD73 concentrations were measured in the supernatants of MDA-MB-231 and 4175TR cells treated with 8 Gy × 3, a radiation regimen similar to that used in patients with breast cancer (32). sCD73 amounts were significantly increased after treatment of MDA-MB-231 with 8 Gy × 3 (**Fig. 3B**) with similar effects on 4175TR cells (Supplementary Fig. S3B).

Next, we explored the effects of radiotherapy on upregulation of the ectonucleotidases that generate adenosine in patients with breast cancer. Given that increased amounts of surface CD73 were associated with increased sCD73 in *in vitro* irradiated breast cancer cells, we measured sCD73 amounts in plasma samples available from 15 patients with metastatic breast cancer who were treated in a clinical study testing the combination of radiotherapy (7.5 Gy × 3) with the

Published OnlineFirst February 11, 2020; DOI: 10.1158/2326-6066.CIR-19-0449

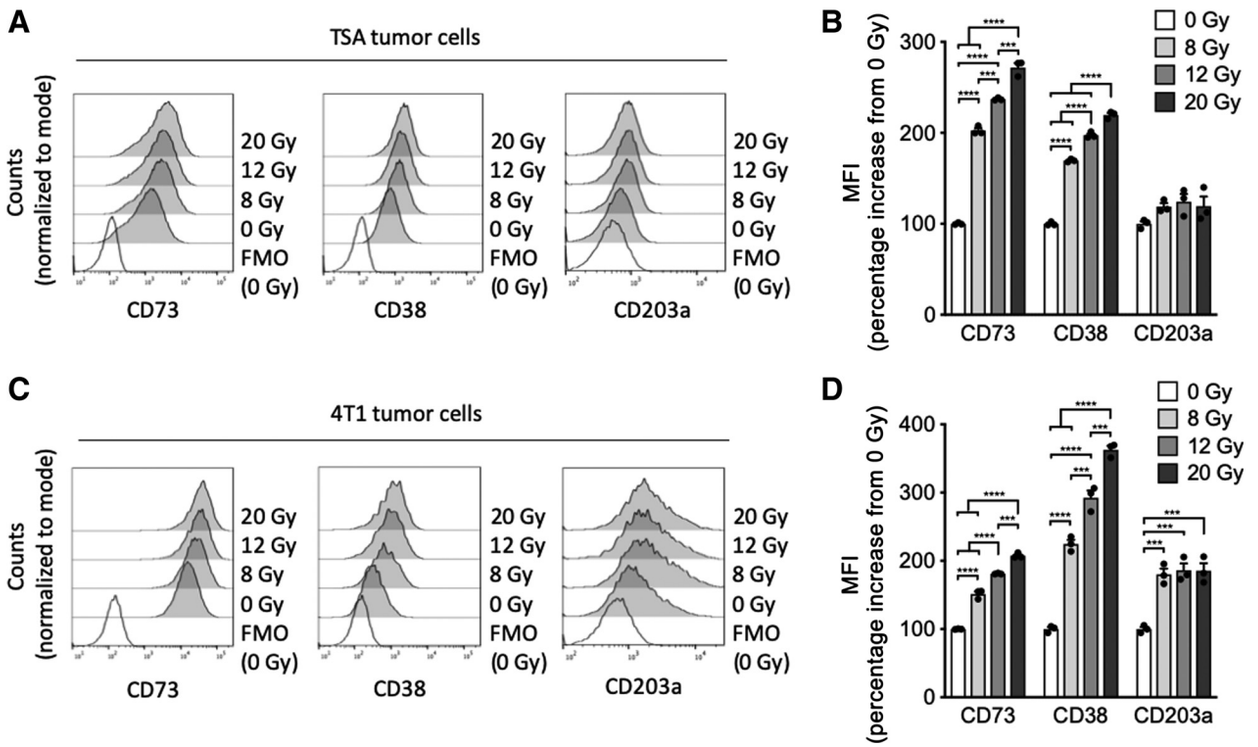

Figure 2.

Radiation increases expression of noncanonical adenosine generation pathway by mouse breast cancer cells. TSA and 4T1 tumor cells were treated with single doses of radiation as indicated and analyzed 24 hours later by flow cytometry. **A** and **B,** Expression of CD73, CD38, and CD203a on TSA tumor cells ($n = 3$ per group). Representative histograms (**A**) and percentage increase in MFI compared with mock-treated cells (0 Gy; **B**). **C** and **D,** Expression of CD73, CD38, and CD203a on 4T1 tumor cells ($n = 3$ per group). Representative histograms (**C**) and percentage increase in MFI compared with mock-treated cells (0 Gy; **D**). All data show mean ± SEM. ANOVA followed by Tukey test (***, $P < 0.001$; ****, $P < 0.0001$). FMO, fluorescence minus one.

TGFβ-neutralizing antibody fresolimumab (32). Six patients had TNBC, 7 patients had hormone receptor–positive (HR^+) $HER2^-$ breast cancer, 1 had HR^+HER2^+ breast cancer, and 1 had HR^-HER2^+ breast cancer. No objective responses were observed in this trial, although patients randomized to the higher dose of fresolimumab experienced better survival (32). Concentrations of sCD73 were significantly increased from baseline at week 2, shortly after completion of radiotherapy (**Fig. 3C**). This increase was similar in patients receiving 1 mg/kg or 10 mg/kg fresolimumab ($P = 0.732$). Although an effect of fresolimumab on sCD73 concentrations cannot be excluded, TGFβ enhances expression of CD73 (36), thus it is unlikely that TGFβ blockade is responsible for increased sCD73. Five of 6 patients with TNBC, but only 3 of 7 patients with HR^+HER2^- breast cancer showed increased sCD73 at week 2 compared with baseline, but the numbers are too small to suggest a differential response dependent on tumor subtype.

Blocking adenosine generation enhances tumor response to 20 Gy radiotherapy

To test the consequences of radiation-induced adenosine generation in the tumor microenvironment, anti-CD73 was administered to mice in conjunction with focal radiotherapy (**Fig. 4A**). A single dose of 20 Gy radiotherapy was administered because this dose induced the most consistent increase in tumor concentration of adenosine *in vivo* in the TSA model (**Fig. 1A**), and the highest amounts of CD73 on TSA cells (**Fig. 2B**). Despite baseline expression of CD73 on TSA cells, CD73 blockade had no significant effect on tumor progression and survival in nonirradiated mice. In combination with radiotherapy, CD73 blockade enhanced tumor response and extended mice survival, with 2 of 7 mice showing complete tumor regression (**Fig. 4B** and **C**). To determine whether the activity of the combination treatment was due to CD73 blockade on the cancer cells and/or the tumor stroma, TSA cells were transduced with a doxycycline-inducible shRNA construct targeting CD73 (TSA^{shCD73}). After knockdown was confirmed (Supplementary Fig. S4A), TSA^{shCD73} and TSA cells expressing a nonsilencing construct (TSA^{shNS}) were implanted into mice. Six days later mice were given doxycycline to induce CD73 knockdown followed by treatment with 20 Gy radiotherapy (Supplementary Fig. S4B). Without radiation, CD73 knockdown did not affect tumor growth. With radiation (20 Gy), CD73 knockdown improved tumor response to the same extent as antibody-mediated blockade of CD73 in mice bearing TSA^{shNS} tumors (Supplementary Fig. S4C). Addition of anti-CD73 to mice bearing TSA^{shCD73} and treated with radiotherapy did not further improve tumor control or mice survival (Supplementary Fig. S4D), indicating that CD73 expressed by the cancer cells is the target limiting the response to radiotherapy.

To dissect the mechanisms responsible for tumor control by the combination of radiotherapy and CD73 blockade, the immune infiltrate was analyzed a week after beginning of treatment. CD73 blockade alone had no effect, but when used with 20 Gy radiotherapy, it increased the cDC1 subset (identified by CD8α expression) of intratumoral DCs and their expression of the maturation marker CD86 (**Fig. 4D** and **E**). These results were confirmed using the cDC1 marker

Published OnlineFirst February 11, 2020; DOI: 10.1158/2326-6066.CIR-19-0449

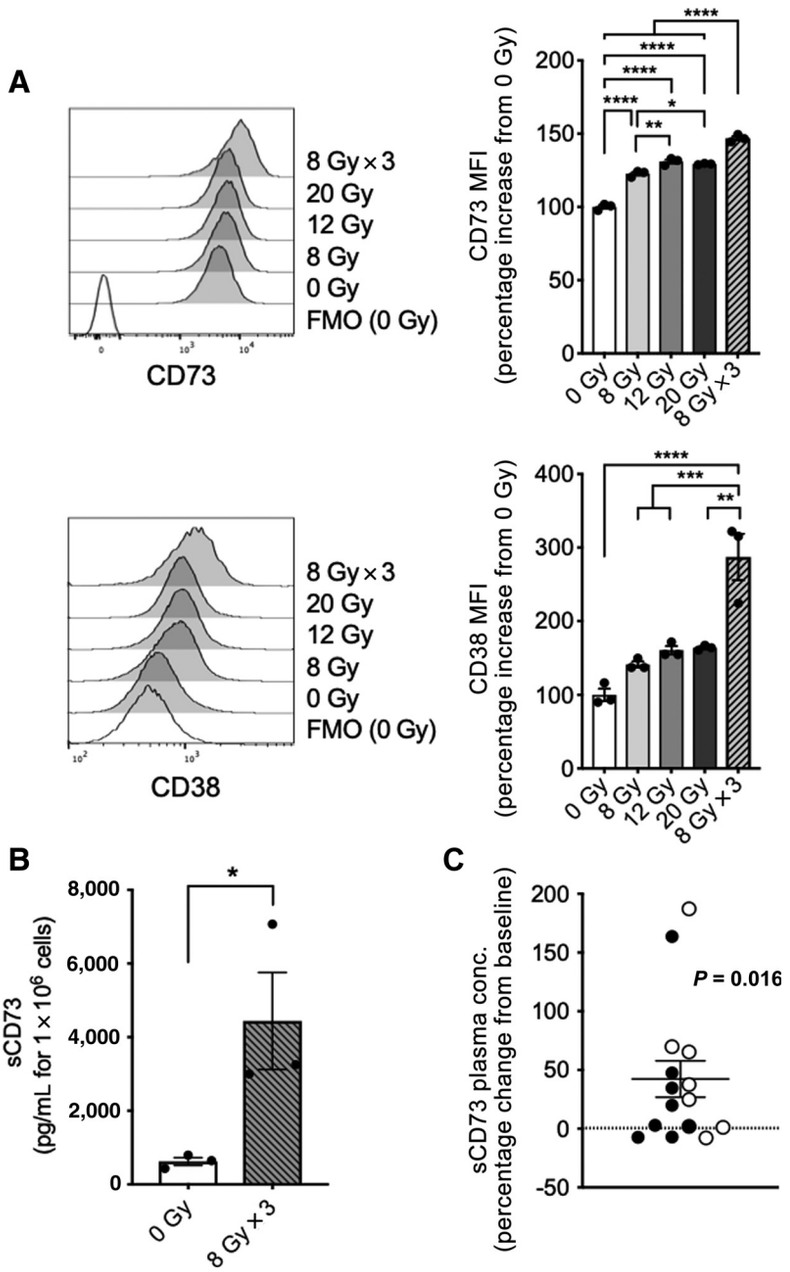

Figure 3.

Radiation-induced upregulation of adenosine-generating ectonucleotidases in human breast cancer. **A,** Representative histograms depicting expression of CD73 (top) and CD38 (bottom) on MDA-MB-231 cells 24 hours posttreatment with radiation as indicated. Bar graphs show percentage increase in MFI compared with mock-treated cells (0 Gy; $n = 3$). ANOVA followed by Tukey test. FMO, fluorescence minus one. **B,** sCD73 in supernatants from MDA-MB-231 cells treated with radiation as indicated measured 24 hours after last radiation dose. $n = 3$, unpaired t test. **C,** Percentage change in concentration (conc.) of sCD73 in plasma samples from patients with breast cancer ($n = 15$) 2 weeks following treatment with radiotherapy (7.5 Gy × 3) and fresolimumab [1 mg/kg (filled circles) or 10 mg/kg (open circles)] compared with baseline sCD73 concentration. Each symbol represents a patient ($n = 15$). One-sample t test. All data show mean ± SEM (*, $P < 0.05$; **, $P < 0.01$; ***, $P < 0.001$; ****, $P < 0.0001$).

CD103 and CD40 as a maturation marker (Supplementary Fig. S5). Analysis of the T-cell compartment revealed an increase in $CD8^+$ T cells in tumors of mice treated with 20 Gy and CD73 blockade (**Fig. 4F**). Expression of CD69, a marker of T-cell activation and tissue-resident differentiation, was enhanced in $CD8^+$ T cells within irradiated tumors, and further enhanced by CD73 blockade (**Fig. 4G**). Tregs were significantly increased by 20 Gy radiotherapy, consistent with the previously observed increase in Treg after tumor irradiation with a similar single radiotherapy dose (37), but this increase was abrogated by CD73 blockade (**Fig. 4H**). The ratio of $CD8^+$ T cells to Tregs, a parameter associated with effective tumor rejection in response to immunotherapy (38), was significantly increased only in tumors of mice treated with radiotherapy and CD73 blockade (**Fig. 4I**).

Next, we investigated the kinetics of DC infiltration in irradiated tumors in response to CD73 blockade (Supplementary Fig. S6). A significant change in cDC1 numbers over time was seen only in tumors of mice treated with both 20 Gy radiation and CD73 blockade: change was evident at day 4 and increased at day 6 (Supplementary Fig. S6B). Immunostaining of tumor sections confirmed the presence of cDC1 cells inside the tumor and showed that some DCs formed clusters with T cells (Supplementary Fig. S6C and S6D).

Overall, these results indicate that targeting CD73 in mice bearing TSA tumors has no effect by itself but acts in synergy with radiotherapy to improve tumor infiltration by cDC1 and T cells and to promote tumor rejection.

Published OnlineFirst February 11, 2020; DOI: 10.1158/2326-6066.CIR-19-0449

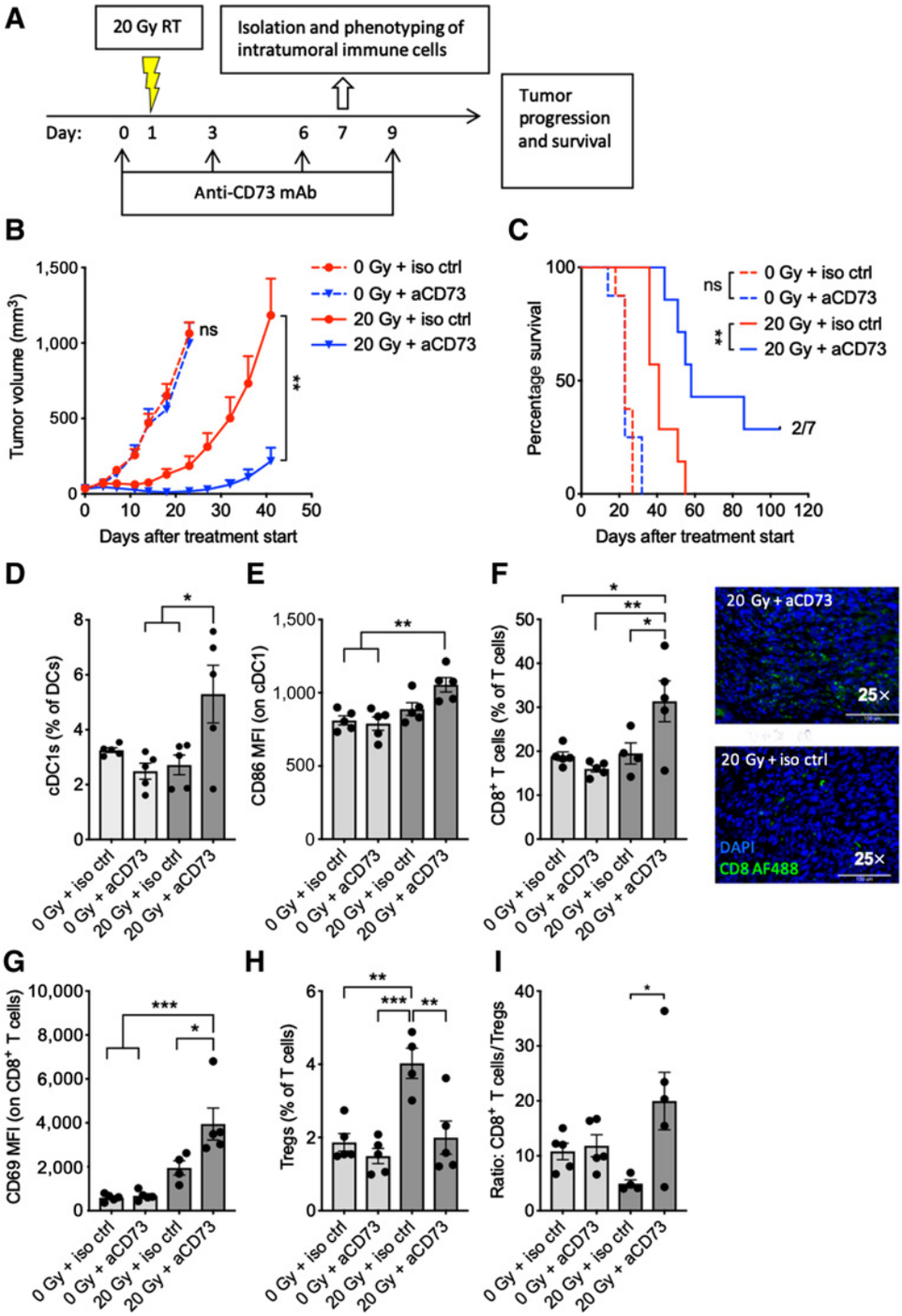

Figure 4.

Blocking CD73 improved the response to 20 Gy radiotherapy, increased tumor infiltration by DCs, and enhanced $CD8^+$ T-cell/Treg ratio. **A,** Tumor treatment schema. Mice bearing TSA tumors were treated with 20 Gy radiotherapy (RT) and/or anti-CD73 or isotype control antibody as indicated. Some mice were sacrificed on day 7 for flow cytometric analysis of intratumoral immune cells ($n = 4$–5 per group). The remaining mice ($n = 7$ per group) were followed for tumor growth (**B**) and survival (**C**). Effect of anti-CD73 on tumor progression as assessed by repeated measure ANOVA in mock-treated mice (0 Gy) between day 0 (treatment start) and day 23 and in radiotherapy-treated mice (20 Gy) between day 0 and day 41. Log-rank test was used to assess effect of anti-CD73 on mouse survival for mice treated with the same radiotherapy treatment. The experiment was performed twice with similar results. **D,** Frequency of cDC1s ($CD8\alpha^+$) among DCs. **E,** MFI of CD86 by DCs. **F,** Percentage of $CD8^+$ T cells among T cells (left) and tumor infiltration of $CD8^+$ T cells in tumor sections stained as indicated (25× magnification; right). **G,** MFI of CD69 on $CD8^+$ T cells. **H,** Percentage of Tregs among T cells. **I,** Ratio of $CD8^+$ T cells to Tregs. Experiment was repeated two to three times with similar results. ANOVA followed by Tukey test. All data show mean ± SEM (*, $P < 0.05$; **, $P < 0.01$; ***, $P < 0.001$; ns, not significant). aCD73, anti-CD73; iso ctrl, isotype control.

Published OnlineFirst February 11, 2020; DOI: 10.1158/2326-6066.CIR-19-0449

cDC1s induce antitumor immune responses to treatment with CD73 blockade and 20 Gy radiotherapy

Radiotherapy-induced infiltration of TSA tumors by cDC1s primes antitumor CD8$^+$ T-cell responses to 8 Gy × 3 radiotherapy, but does not occur when tumors are treated with a single dose of 20 Gy radiotherapy due to poor induction of IFN-I by this radiotherapy dose (9). Given the enrichment of cDC1 and CD8$^+$ T cells in TSA tumors treated with the combination of 20 Gy radiotherapy and CD73

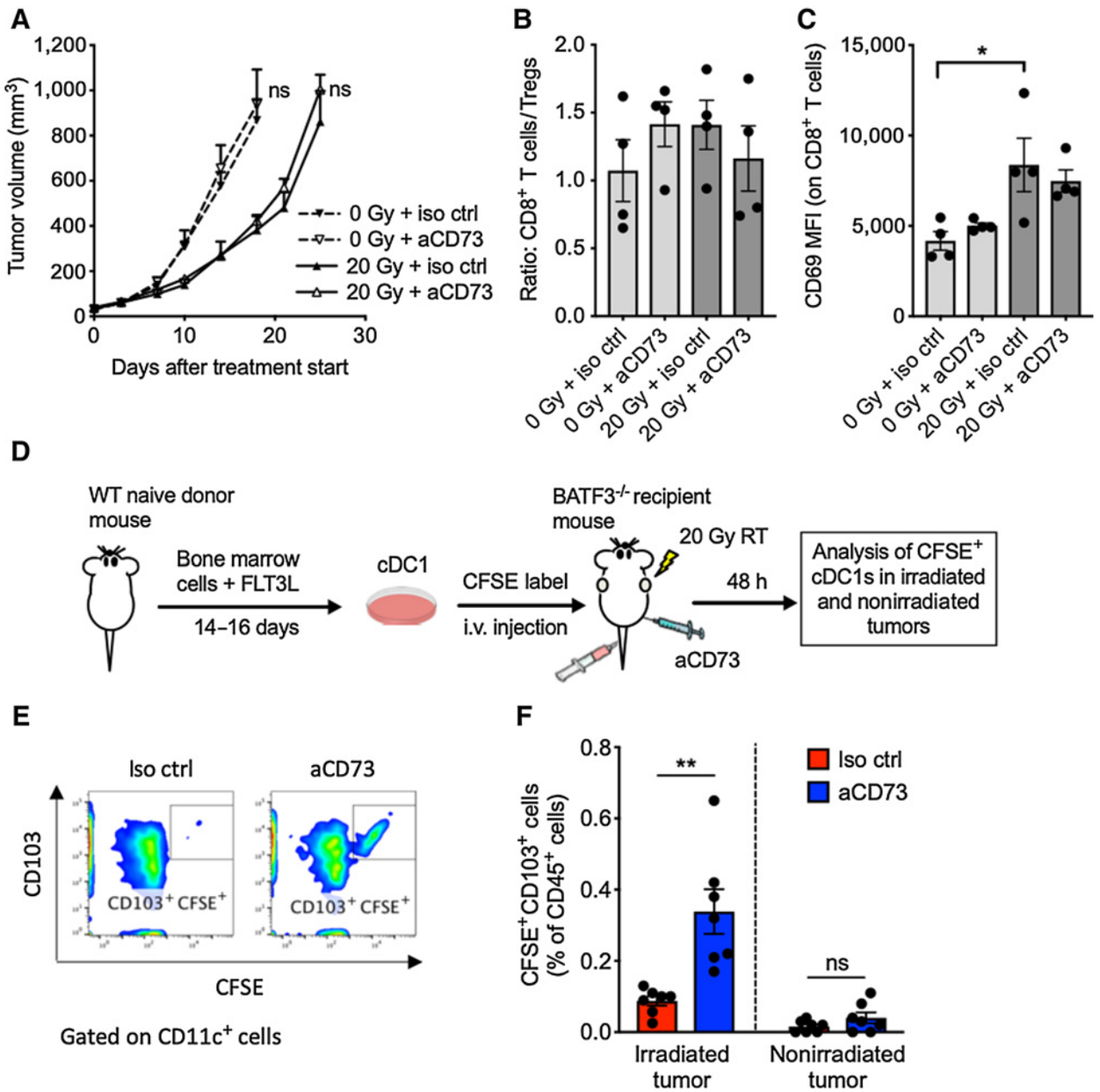

Figure 5.

Synergy of 20 Gy radiotherapy with CD73 blockade depends on cDC1. Batf3$^{-/-}$ mice were inoculated subcutaneously with TSA cells and treated with 20 Gy radiotherapy and anti-CD73 or isotype control as in **Fig. 4A**. **A,** Mice were followed for tumor growth ($n = 5$ per group). Effect of anti-CD73 on tumor progression was assessed by repeated measure ANOVA in mock-treated mice (0 Gy) between day 0 (treatment start) and day 18 and in radiotherapy-treated mice (20 Gy) between day 0 and day 25. **B** and **C,** Some mice were sacrificed on day 7 for analysis of intratumoral immune cells ($n = 4$). Ratio of CD8$^+$ T cells to Tregs (**B**) and MFI of CD69 on CD8$^+$ T cells (**C**). ANOVA followed by Tukey test. **D,** Experimental schema for the cDC1 adoptive transfer. Bone marrow cells from WT mice were cultured with FLT3L and GM-CSF to generate CD103$^+$ cDC1s. cDC1s were labeled with CFSE before intravenous injections into Batf3$^{-/-}$mice bearing two TSA tumors, 6 hours after irradiation of one tumor with 20 Gy and anti-CD73 or control mAb administration. Irradiated and nonirradiated tumors were harvested 48 hours (h) after adoptive transfer for flow cytometry analysis. RT, radiotherapy. **E,** Representative dot plots of intratumoral CD11c$^+$ cells analyzed for expression of CFSE and CD103. **F,** Frequency of CFSE$^+$CD103$^+$ cDC1s among total viable leukocytes in irradiated tumors and nonirradiated tumors ($n = 7$ per group), Welch t test. All data show mean ± SEM (*, $P < 0.01$; **, $P < 0.01$; ns, not significant). aCD73, anti-CD73; iso ctrl, isotype control.

Published OnlineFirst February 11, 2020; DOI: 10.1158/2326-6066.CIR-19-0449

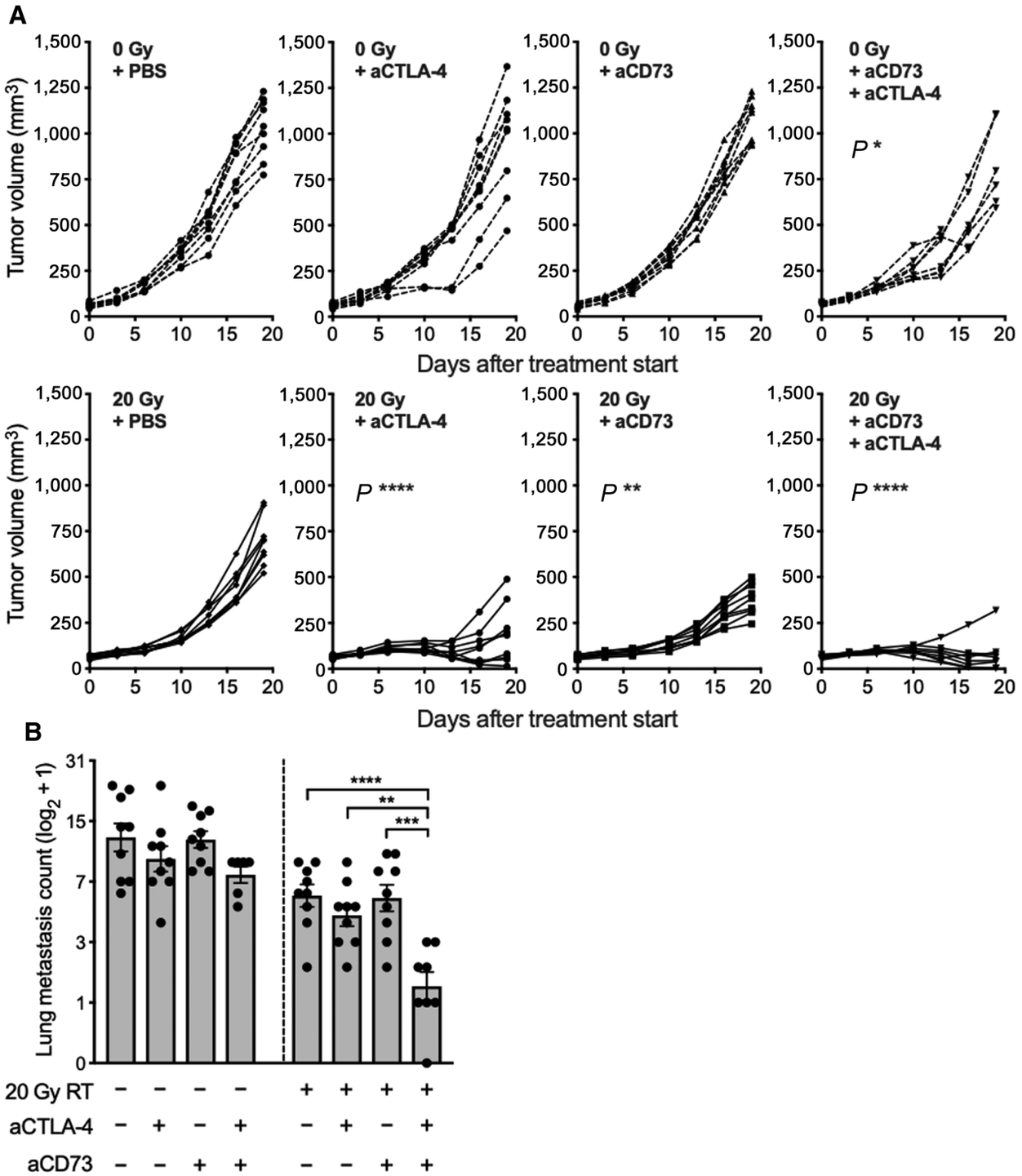

Figure 6.

CD73 blockade in combination with anti–CTLA-4 enhanced 4T1 tumor response to radiotherapy and inhibited lung metastases. BALB/c mice were inoculated subcutaneously with 4T1 cells in the right flank. Treatment with anti-CD73 was started when average tumor volumes approached 40 to 60 mm^3 (day 0) and repeated on days 3, 6, and 9. Radiotherapy was given as a single 20 Gy dose to the tumor on day 1. Anti–CTLA-4 was administered on days 1, 4, and 7. **A** and **B,** Mice were followed for tumor growth and euthanized on day 19 for assessment of lung metastases. **A,** Tumor progression in individual mice. Statistical significance was assessed by repeated measure ANOVA. Asterisks indicate *P* values for the comparison of each treatment group versus PBS-treated controls for mice treated with the same radiotherapy treatment. **B,** Number of lung metastases on day 19 after treatment start ($n = 6$–9 per group). Metastases counts were $\log_2$ transformed. ANOVA followed by Tukey test. All data show mean ± SEM (*, $P < 0.05$; **, $P < 0.01$; ***, $P < 0.001$; ****, $P < 0.0001$). aCD73, anti-CD73; aCTLA-4, anti–CTLA-4.

Published OnlineFirst February 11, 2020; DOI: 10.1158/2326-6066.CIR-19-0449

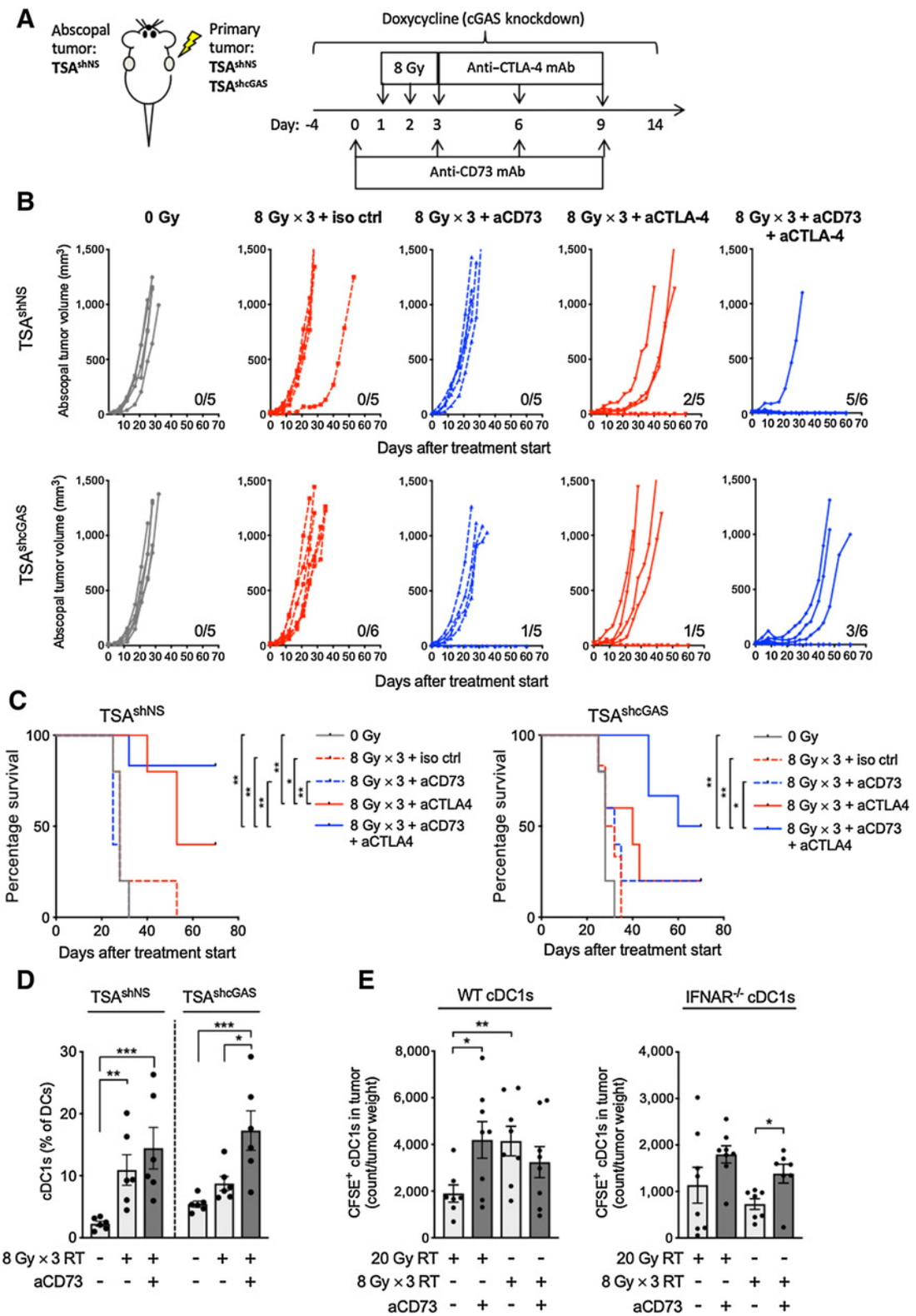

Published OnlineFirst February 11, 2020; DOI: 10.1158/2326-6066.CIR-19-0449

blockade (**Fig. 4D** and **F**; Supplementary Fig. S5), we asked whether the synergy of 20 Gy and CD73 blockade was cDC1 dependent. We used Batf3$^{-/-}$ mice that lack cDC1 as recipient of TSA cells. The synergy between 20 Gy radiotherapy and CD73 blockade was abrogated in Batf3$^{-/-}$ mice (**Fig. 5A**). Consistent with the inability of these mice to activate antitumor CD8$^+$ T cells, the intratumoral CD8$^+$T-cell: Treg ratio was not increased in Batf3$^{-/-}$ mice treated with 20 Gy and CD73 blockade (**Fig. 5B**). Expression of CD69 by CD8$^+$ T cells was induced by radiotherapy but not further increased by CD73 blockade (**Fig. 5C**), indicating that the effects of CD73 blockade are dependent on cDC1s.

To test the ability of 20 Gy radiotherapy to elicit signals that promote tumor infiltration by cDC1 when CD73 is blocked, we generated cDC1 *ex vivo* by culture of bone marrow cells from WT BALB/c mice with FLT3L and GM-CSF as described previously (30). Obtained cDC1s were labeled with CFSE and injected intravenously into Batf3$^{-/-}$ mice bearing two TSA tumors in opposite flanks 6 hours after irradiation of one tumor with 20 Gy and administration of anti-CD73 (**Fig. 5D**). Forty-eight hours after injection, both tumors were harvested and analyzed for infiltration by the adoptively transferred cDC1s (CFSE$^+$CD103$^+$). CD73 blockade significantly enhanced cDC1 infiltration in irradiated but not untreated tumors (**Fig. 5E** and **F**). These results indicate that cDC1 homing to TSA tumors requires chemotactic and/or survival signals induced by radiotherapy together with blockade of adenosine generation.

CD73 blockade enhances abscopal responses in mice treated with 20 Gy radiotherapy and CTLA-4 blockade

4T1 is a poorly immunogenic model of TNBC resistant to ICB that seeds spontaneous metastases to the lungs; metastases are present by the time the primary tumor is palpable (39). We have previously shown that radiotherapy used at 8 to 12 Gy dose per fraction, delivered in consecutive days 2–3 times, is synergistic with CTLA-4 and induces CD8$^+$T-cell responses that control nonirradiated lung metastases (40). Similarly to TSA cells, 4T1 cells do not show radiotherapy-induced IFN-I production or priming of antitumor CD8$^+$ T cells when treated with single-dose 20 Gy radiotherapy (9). Because CD73 was upregulated on 4T1 cells by radiotherapy (**Fig. 2C** and **D**), we asked whether CD73 blockade could improve the local and systemic response of mice bearing 4T1 tumors treated with 20 Gy radiotherapy. Blockade of CD73, beginning when tumors were palpable, had no effect on the primary tumor or lung metastases (**Fig. 6A** and **B**). When used with 20 Gy radiotherapy, CD73 blockade enhanced control of the irradiated tumor but not of lung metastases, suggesting that the immune response elicited by 20 Gy + CD73 blockade was not systemically effective. Therefore, we tested whether addition of CTLA-4 blockade could improve the control of the nonirradiated metastases in the lungs of mice treated with 20 Gy + CD73 blockade. The double blockade of CD73 and CTLA-4 had no effect without radiotherapy, but resulted in a significant decrease in lung metastases when combined with 20 Gy radiotherapy (**Fig. 6B**).

These results confirm the benefits of blocking adenosine generation to improve responses to radiotherapy. In addition, they show that CD73 blockade induces systemic antitumor immune responses in mice treated with a radiotherapy dose that is otherwise unable to induce abscopal effects in combination with anti–CTLA-4 (9).

CD73 blockade promotes cDC1 recruitment to irradiated tumors and improves abscopal response

cGAS-deficient TSA tumors cannot produce IFN-I in response to 8 Gy × 3 radiotherapy and fail to induce tumor-specific CD8$^+$ T-cell activation and abscopal responses in combination with CTLA-4 blockade (9). Given the ability of CD73 blockade to induce the recruitment of cDC1s to tumors treated with 20 Gy, a radiotherapy dose that does not induce IFN-I (9), we hypothesized that CD73 blockade could complement the lack of IFN-I induction by 8 Gy × 3 radiotherapy when the irradiated tumor was cGAS deficient. To test this hypothesis, we employed an abscopal tumor model in which TSA cells, transduced with doxycycline-inducible TSA^{shcGAS} or a nonsilencing sequence (TSA^{shNS}), are injected in the right flank of WT BALB/c mice (primary tumor) followed by injection of TSA^{shNS} in the contralateral flank (abscopal tumor; ref. 9). Primary tumors were irradiated with 8 Gy × 3, and mice received anti-CD73 and/or anti–CTLA-4 (**Fig. 7A**). As expected, radiotherapy was effective at controlling the irradiated tumors regardless of cGAS expression (Supplementary Fig. S7), but did not induce abscopal responses. Consistently with prior results, CTLA-4 blockade with radiotherapy induced abscopal responses and increased significantly the survival of mice bearing TSA^{shNS} but not TSA^{shcGAS} primary tumors (9). CD73 blockade with radiotherapy did not induce abscopal responses in mice bearing TSA^{shNS} or TSA^{shcGAS} primary tumors (**Fig. 7B**). However, CD73 blockade restored the ability of the combination of 8 Gy × 3 radiotherapy and CTLA-4 blockade to induce abscopal responses and extend survival of mice with TSA^{shcGAS} primary tumors (**Fig. 7B** and **C**). These data indicate that CD73 blockade is insufficient to induce abscopal responses in combination with radiotherapy, but can complement the defective activation of IFN-I by radiotherapy in tumors with downregulated cGAS expression.

Figure 7.

CD73 blockade improved induction of abscopal response upon irradiation of cGAS-deficient tumors and restored impaired recruitment of cDC1s to cGAS-deficient tumors following radiotherapy. **A,** Experimental schema. TSA^{shcGAS} or a TSA^{shNS} was injected in the right flank of WT BALB/c mice (primary tumors). Two days later TSA^{shNS} cells were injected in the contralateral flank (abscopal tumors). Doxycycline was fed to mice once the tumors became palpable (day −4), and treatment started when primary tumors reached a volume of 40 to 60 mm^3 (day 0). Radiotherapy was given in three daily doses of 8 Gy to the primary tumor. Anti-CD73 and anti–CTLA-4 mAbs were administered intraperitoneally as indicated, and mice followed for tumor growth and survival. **B,** Abscopal tumor growth over time. Each line represents an individual mouse (n = 5–6). Numbers indicate the number of mice with complete tumor regression over the total in each group. **C,** Survival in mice bearing primary TSA^{shNS} tumors or TSA^{shcGAS} tumors. Log-rank (Mantel–Cox) test. **D,** WT BALB/c mice were inoculated with primary TSA^{shNS} or TSA^{shcGAS} tumors and treated as above with radiotherapy and CD73 blockade. Tumors were harvested 5 days after last dose of radiotherapy for analysis of percentage of cDC1s (XCR1$^+$CD8α$^+$) among total DCs (n = 6 per group, ANOVA). Experiment was performed twice with similar results. **E,** cDC1s prepared from the bone marrow of WT or Ifnar$^{-/-}$ mice were labeled with CSFE and adoptively transferred into WT BALB/c mice bearing TSA tumors 6 hours after irradiation with 20 Gy × 1 or 8 Gy × 3 and/or anti-CD73 administration. Tumors harvested 48 hours later were evaluated for CFSE-labeled cDC1 infiltration. Bar graphs show the number of CFSE$^+$CD11c$^+$ cells normalized to tumor weight in mice receiving WT cDC1s (left) and Ifnar$^{-/-}$ cDC1s (right; n = 7–8). Welch t test. Data were square root transformed prior to statistical testing. All data show mean ± SEM (*, $P < 0.05$; **, $P < 0.01$; ***, $P < 0.001$). aCD73, anti-CD73; aCTLA-4, anti–CTLA-4; iso ctrl, isotype control; RT, radiotherapy.

Published OnlineFirst February 11, 2020; DOI: 10.1158/2326-6066.CIR-19-0449

Next, we sought to test whether CD73 blockade could promote the recruitment of cDC1s to cGAS-deficient tumors. We analyzed primary TSA^{shNS} and TSA^{shcGAS} tumors from mice treated with or without CD73 blockade for the presence of cDC1s 5 days following completion of 8 Gy × 3 radiotherapy. As expected, 8 Gy × 3 radiotherapy increased cDC1s in TSA^{shNS} tumors but not in TSA^{shcGAS} tumors (**Fig. 7D**; ref. 9). CD73 blockade did not further increase cDC1s in irradiated TSA^{shNS} tumors but restored radiotherapy-induced cDC1 increases in TSA^{shcGAS} tumors (**Fig. 7D**). cDC1 recruitment to tumors treated with 8 Gy × 3 is mediated by IFN-I and requires host expression of the IFN-I receptor (9). To determine whether cDC1 recruitment mediated by radiotherapy in the presence of CD73 blockade was independent from IFN-I, we performed an adoptive transfer experiment. cDC1s were obtained by culture of bone marrow cells derived from $Ifnar1^{-/-}$ mice or from WT mice. After CFSE labeling, cDC1s were injected intravenously into WT mice bearing TSA tumors treated with 20 Gy or 8 Gy × 3 radiotherapy, then, 48 hours later, measured the number of $CFSE^+$ cDC1 cells infiltrating the irradiated tumors by flow cytometry. In-line with previous findings (9), WT cDC1s homed in significantly higher numbers to tumors treated with 8 Gy × 3 than 20 Gy radiotherapy (**Fig. 7E**). In contrast, homing of $Ifnar^{-/-}$ cDC1s to tumors treated with 8 Gy × 3 radiotherapy was not increased. CD73 blockade did not further increase homing of WT cDC1s to tumors treated with 8 Gy × 3, but restored homing of WT cDC1s to tumors treated with 20 Gy and restored homing of the $Ifnar^{-/-}$ cDC1 to tumors treated with either 8 Gy × 3 radiotherapy or 20 Gy radiotherapy (**Fig. 7E**). Thus, when IFN-I–driven recruitment of cDC1s to tumors is hampered, an alternative pathway for cDC1 recruitment can be activated by radiotherapy and regulated by adenosine.

Our results show that CD73 regulates *in situ* vaccination by radiotherapy and radiotherapy enhances responses of breast cancer to ICB.

Discussion

Recruitment of cDC1s to the tumor is essential for the development of spontaneous antitumor $CD8^+$ T cells, and cDC1 exclusion is one of the mechanisms responsible for the "cold" immunologic phenotype characteristic of tumors resistant to ICB therapy (41–43). Focal radiotherapy enhances responses of poorly immunogenic "cold" tumors to ICB therapy at least in part by promoting recruitment and maturation of cDC1s (9). Radiotherapy-induced IFN-I plays a role in priming of antitumor T cells by radiotherapy; data suggest that this mechanism is clinically relevant (6, 8, 9, 44). IFN-I provides a signal for cDC1 recruitment to the tumor (41). We and others have demonstrated that IFN-I production by cancer cells is mediated by radiotherapy-induced activation of the cGAS/STING pathway by self DNA that accumulates in the cytosol (9, 10). Here, we describe an alternative pathway for the recruitment of cDC1s to irradiated tumors that is independent of IFN-I and is regulated by CD73.

Blockade of CD73 had no effect on tumor growth by itself or in combination with anti–CTLA-4 in two tumor models of metastatic breast cancer. However, when combined with a radiotherapy dose of 20 Gy, which is unable to induce IFN-I production by the irradiated cancer cells (9), CD73 blockade improved control of the irradiated tumor and, in combination with CTLA-4 blockade, nonirradiated lung metastases (9). Likewise, when cGAS-deficient TSA tumors were treated with 8 Gy × 3 radiotherapy and CTLA-4 blockade, CD73 blockade restored the induction of abscopal responses and improved mice survival. These results have clinical implications as many tumors epigenetically downregulate expression of cGAS and/or STING and may not be able to produce IFN-I in response to radiotherapy (12). In a clinical trial testing the combination of radiotherapy and the anti–CTLA-4 antibody ipilimumab in metastatic lung patients, we found that increased serum IFN-I after radiotherapy predicted an abscopal responses (6). Reasons for the failure of radiotherapy to induce IFN-I in nonresponding patients are unclear, but it is possible that downregulation of cGAS/STING hindered the response, and that these patients could have benefited from treatment with CD73-blocking antibodies.

Radiotherapy-induced factors that promote tumor infiltration by cDC1s in the absence of IFN-I remain to be defined. Extracellular nucleotides mediate chemotaxis of DCs (45), and ATP released following chemotherapy mediated DC recruitment to the tumor *in vivo* (15, 46). *In vitro*, radiotherapy induced dose-dependent release of ATP by tumor cells (47), suggesting that ATP could mediate cDC1 recruitment to irradiated tumors. Conversion of ATP to adenosine may also affect the balance of activating and suppressive signals that regulate the retention, activation, and survival of cDC1s within the irradiated tumor microenvironment (48). Further studies are required to define the effect of CD73 blockade on these processes in the irradiated tumor microenvironment.

Expression of CD73 on cancer cells inhibits tumor rejection by adoptively transferred antitumor T cells (49). We found that CD73 expressed on mouse and human breast cancer cells is upregulated by radiation. Knockdown of CD73 did not affect TSA tumor in the absence of radiotherapy, but enhanced tumor control in concert with radiotherapy. Thus, radiation-induced T-cell activation as dependent on cDC1 is necessary, an interpretation supported by loss of the therapeutic synergy between CD73 blockade and radiotherapy in $Batf3^{-/-}$ mice.

Radiotherapy increased expression of CD38 by mouse and human breast cancer cells, suggesting that the noncanonical pathway may contribute to the generation of adenosine induced by radiotherapy. CD38 has been implicated in generation of adenosine in melanoma, and upregulation of CD38 on tumor cells plays a role in resistance to anti–PD-1/PD-L1 therapy (17, 25). Together with a known role of radiotherapy in disrupting NAD^+ metabolism, these data support the hypothesis that NAD^+ may be a source of adenosine in the irradiated tumor (50).

Expression of CD73 in TNBC is associated with a poor prognosis and poor response to neoadjuvant chemotherapy (22). Our preclinical data indicate that CD73 expression also reduces breast cancer response to radiotherapy, thus precluding the synergy of radiotherapy with ICB therapy in tumors unable to activate IFN-I. The observed increase in plasma sCD73 after radiotherapy in patients with metastatic breast cancer supports the concept that this pathway should be targeted in the clinic to improve responses, especially when radiotherapy is used in combination with ICB. sCD73 expression in patients with breast cancer and its modulation by radiotherapy should be explored as a potential biomarker predictive of response.

In summary, we have identified a role for the adenosinergic pathway in regulating radiotherapy-induced *in situ* vaccination by limiting cDC1 infiltration in conditions of suboptimal IFN-I induction by radiotherapy. Clinical trials are underway to assess safety and efficacy of CD73-blocking antibodies alone or in combination with ICB in patients with advanced solid tumors (26). Our findings provide the rationale for testing CD73 blockade in patients who carry $cGAS/STING^-$ tumors or show upregulation of sCD73 following radiotherapy to determine whether CD73 blockade can enhance responses to ICB.

Disclosure of Potential Conflicts of Interest

S.C. Formenti's daughter is an attorney for Pfizer. S.C. Formenti reports receiving commercial research grants from Bristol-Myers Squibb, Varian, Merck, Regeneron, and Eisai and speakers bureau honoraria from Varian, Eisai, AstraZeneca, Merck, Viewray, Bayer, and EMD Serono. S. Demaria is a scientific advisory board member for Lytix Biopharma, is an ad hoc consultant for AstraZeneca, Mersana Therapeutics, and EMD Serono, and reports receiving commercial research grants from Lytix Biopharma and Nanobiotix. No potential conflicts of interest were disclosed by the other authors.

Authors' Contributions

Conception and design: E. Wennerberg, S.S. Gross, S.C. Formenti, S. Demaria
Development of methodology: E. Wennerberg, S.C. Formenti
Acquisition of data (provided animals, acquired and managed patients, provided facilities, etc.): E. Wennerberg, S. Spada, N.-P. Rudqvist, C. Lhuillier, S. Gruber, Q. Chen, F. Zhang, S.S. Gross
Analysis and interpretation of data (e.g., statistical analysis, biostatistics, computational analysis): E. Wennerberg, S. Spada, N.-P. Rudqvist, C. Lhuillier, S. Gruber, Q. Chen, X.K. Zhou, S.S. Gross
Writing, review, and/or revision of the manuscript: E. Wennerberg, X.K. Zhou, S.C. Formenti, S. Demaria
Administrative, technical, or material support (i.e., reporting or organizing data, constructing databases): S.C. Formenti
Study supervision: S. Demaria
Other (use of mouse irradiator, NIH/NCI RR0267619-01): S.C. Formenti

Acknowledgments

We thank Dr. Fabio Malavasi for helpful discussions, Bruce Cronstein for adenosine measurement help, Barbara Maier and Miriam Merad for cDC1 generation and identification protocols, and Andreas Lundqvist for critically reviewing the article. This study was supported by the U.S. Department of Defense, Breast Cancer Research Program Breakthrough Fellowship Award W81XWH-17-1-0029 to E. Wennerberg and Multi-Team Award W81XWH-11-1-0530 to S.C. Formenti, and by NIH R01 CA201246 to S. Demaria. Additional funding was provided by grants from the Breast Cancer Research Foundation (BCRF-16-054 and BCRF-17-053) to S. Demaria and S.C. Formenti.

The costs of publication of this article were defrayed in part by the payment of page charges. This article must therefore be hereby marked *advertisement* in accordance with 18 U.S.C. Section 1734 solely to indicate this fact.

Received June 18, 2019; revised December 1, 2019; accepted February 4, 2020; published first February 11, 2020.

References

1. Ribas A, Wolchok JD. Cancer immunotherapy using checkpoint blockade. Science 2018;359:1350–5.
2. Sharma P, Allison JP. The future of immune checkpoint therapy. Science 2015; 348:56–61.
3. Demaria S, Golden EB, Formenti SC. Role of local radiation therapy in cancer immunotherapy. JAMA Oncol 2015;1:1325–32.
4. Kang J, Demaria S, Formenti S. Current clinical trials testing the combination of immunotherapy with radiotherapy. J Immunother Cancer 2016;4:51.
5. Twyman-Saint Victor C, Rech AJ, Maity A, Rengan R, Pauken KE, Stelekati E, et al. Radiation and dual checkpoint blockade activate non-redundant immune mechanisms in cancer. Nature 2015;520:373–7.
6. Formenti SC, Rudqvist NP, Golden E, Cooper B, Wennerberg E, Lhuillier C, et al. Radiotherapy induces responses of lung cancer to CTLA-4 blockade. Nat Med 2018;24:1845–51.
7. Wennerberg E, Lhuillier C, Vanpouille-Box C, Pilones KA, Garcia-Martinez E, Rudqvist NP, et al. Barriers to radiation-induced in situ tumor vaccination. Front Immunol 2017;8:229.
8. Burnette BC, Liang H, Lee Y, Chlewicki L, Khodarev NN, Weichselbaum RR, et al. The efficacy of radiotherapy relies upon induction of type i interferon-dependent innate and adaptive immunity. Cancer Res 2011;71: 2488–96.
9. Vanpouille-Box C, Alard A, Aryankalayil MJ, Sarfraz Y, Diamond JM, Schneider RJ, et al. DNA exonuclease Trex1 regulates radiotherapy-induced tumour immunogenicity. Nat Commun 2017;8:15618.
10. Harding SM, Benci JL, Irianto J, Discher DE, Minn AJ, Greenberg RA. Mitotic progression following DNA damage enables pattern recognition within micronuclei. Nature 2017;548:466–70.
11. Hildner K, Edelson BT, Purtha WE, Diamond M, Matsushita H, Kohyama M, et al. Batf3 deficiency reveals a critical role for CD8alpha+ dendritic cells in cytotoxic T cell immunity. Science 2008;322:1097–100.
12. Konno H, Yamauchi S, Berglund A, Putney RM, Mule JJ, Barber GN. Suppression of STING signaling through epigenetic silencing and missense mutation impedes DNA damage mediated cytokine production. Oncogene 2018;37:2037–51.
13. Golden EB, Apetoh L. Radiotherapy and immunogenic cell death. Semin Radiat Oncol 2015;25:11–7.
14. Aymeric L, Apetoh L, Ghiringhelli F, Tesniere A, Martins I, Kroemer G, et al. Tumor cell death and ATP release prime dendritic cells and efficient anticancer immunity. Cancer Res 2010;70:855–8.
15. Saez PJ, Vargas P, Shoji KF, Harcha PA, Lennon-Dumenil AM, Saez JC. ATP promotes the fast migration of dendritic cells through the activity of pannexin 1 channels and P2X7 receptors. Sci Signal 2017;10. pii: eaah7107.
16. Young A, Mittal D, Stagg J, Smyth MJ. Targeting cancer-derived adenosine: new therapeutic approaches. Cancer Discov 2014;4:879–88.
17. Morandi F, Morandi B, Horenstein AL, Chillemi A, Quarona V, Zaccarello G, et al. A non-canonical adenosinergic pathway led by CD38 in human melanoma cells induces suppression of T cell proliferation. Oncotarget 2015;6:25602–18.
18. Horenstein AL, Chillemi A, Zaccarello G, Bruzzone S, Quarona V, Zito A, et al. A CD38/CD203a/CD73 ectoenzymatic pathway independent of CD39 drives a novel adenosinergic loop in human T lymphocytes. Oncoimmunology 2013;2: e26246.
19. Ohta A, Gorelik E, Prasad SJ, Ronchese F, Lukashev D, Wong MK, et al. A2A adenosine receptor protects tumors from antitumor T cells. Proc Natl Acad Sci U S A 2006;103:13132–7.
20. Novitskiy SV, Ryzhov S, Zaynagetdinov R, Goldstein AE, Huang Y, Tikhomirov OY, et al. Adenosine receptors in regulation of dendritic cell differentiation and function. Blood 2008;112:1822–31.
21. Zarek PE, Huang CT, Lutz ER, Kowalski J, Horton MR, Linden J, et al. A2A receptor signaling promotes peripheral tolerance by inducing T-cell anergy and the generation of adaptive regulatory T cells. Blood 2008;111:251–9.
22. Loi S, Pommey S, Haibe-Kains B, Beavis PA, Darcy PK, Smyth MJ, et al. CD73 promotes anthracycline resistance and poor prognosis in triple negative breast cancer. Proc Natl Acad Sci U S A 2013;110:11091–6.
23. Jiang T, Xu X, Qiao M, Li X, Zhao C, Zhou F, et al. Comprehensive evaluation of NT5E/CD73 expression and its prognostic significance in distinct types of cancers. BMC Cancer 2018;18:267.
24. Buisseret L, Pommey S, Allard B, Garaud S, Bergeron M, Cousineau I, et al. Clinical significance of CD73 in triple-negative breast cancer: multiplex analysis of a phase III clinical trial. Ann Oncol 2018;29:1056–62.
25. Chen L, Diao L, Yang Y, Yi X, Rodriguez BL, Li Y, et al. CD38-mediated immunosuppression as a mechanism of tumor cell escape from PD-1/PD-L1 blockade. Cancer Discov 2018;8:1156–75.
26. Allard D, Chrobak P, Allard B, Messaoudi N, Stagg J. Targeting the CD73-adenosine axis in immuno-oncology. Immunol Lett 2019;205:31–9.
27. Aslakson CJ, Miller FR. Selective events in the metastatic process defined by analysis of the sequential dissemination of subpopulations of a mouse mammary tumor. Cancer Res 1992;52:1399–405.
28. Rosato A, Santa SD, Zoso A, Giacomelli S, Milan G, Macino B, et al. The cytotoxic T-lymphocyte response against a poorly immunogenic mammary adenocarcinoma is focused on a single immunodominant class I epitope derived from the gp70 Env product of an endogenous retrovirus. Cancer Res 2003;63:2158–63.
29. Lutz MB, Kukutsch N, Ogilvie AL, Rossner S, Koch F, Romani N, et al. An advanced culture method for generating large quantities of highly pure dendritic cells from mouse bone marrow. J Immunol Methods 1999;223:77–92.
30. Mayer CT, Ghorbani P, Nandan A, Dudek M, Arnold-Schrauf C, Hesse C, et al. Selective and efficient generation of functional Batf3-dependent CD103+ dendritic cells from mouse bone marrow. Blood 2014;124:3081–91.

Published OnlineFirst February 11, 2020; DOI: 10.1158/2326-6066.CIR-19-0449

31. Chen Q, Deeb RS, Ma Y, Staudt MR, Crystal RG, Gross SS. Serum metabolite biomarkers discriminate healthy smokers from COPD smokers. PLoS One 2015; 10:e0143937.
32. Formenti SC, Lee P, Adams S, Goldberg JD, Li X, Xie MW, et al. Focal irradiation and systemic TGFbeta blockade in metastatic breast cancer. Clin Cancer Res 2018;24:2493–504.
33. Hasko G, Cronstein BN. Adenosine: an endogenous regulator of innate immunity. Trends Immunol 2004;25:33–9.
34. Morello S, Capone M, Sorrentino C, Giannarelli D, Madonna G, Mallardo D, et al. Soluble CD73 as biomarker in patients with metastatic melanoma patients treated with nivolumab. J Transl Med 2017;15:244.
35. Airas L, Niemela J, Salmi M, Puurunen T, Smith DJ, Jalkanen S. Differential regulation and function of CD73, a glycosyl-phosphatidylinositol-linked 70-kD adhesion molecule, on lymphocytes and endothelial cells. J Cell Biol 1997;136: 421–31.
36. Regateiro FS, Cobbold SP, Waldmann H. CD73 and adenosine generation in the creation of regulatory microenvironments. Clin Exp Immunol 2013;171:1–7.
37. Schaue D, Ratikan JA, Iwamoto KS, McBride WH. Maximizing tumor immunity with fractionated radiation. Int J Radiat Oncol Biol Phys 2012; 83:1306–10.
38. Quezada SA, Peggs KS, Curran MA, Allison JP. CTLA4 blockade and GM-CSF combination immunotherapy alters the intratumor balance of effector and regulatory T cells. J Clin Invest 2006;116:1935–45.
39. Pulaski BA, Ostrand-Rosenberg S. Mouse 4T1 breast tumor model. Curr Protoc Immunol 2001;Chapter 20:Unit 20.2.
40. Demaria S, Kawashima N, Yang AM, Devitt ML, Babb JS, Allison JP, et al. Immune-mediated inhibition of metastases after treatment with local radiation and CTLA-4 blockade in a mouse model of breast cancer. Clin Cancer Res 2005; 11:728–34.
41. Diamond MS, Kinder M, Matsushita H, Mashayekhi M, Dunn GP, Archambault JM, et al. Type I interferon is selectively required by dendritic cells for immune rejection of tumors. J Exp Med 2011;208:1989–2003.
42. Spranger S, Bao R, Gajewski TF. Melanoma-intrinsic beta-catenin signalling prevents anti-tumour immunity. Nature 2015;523:231–5.
43. Sharma P, Allison JP. Immune checkpoint targeting in cancer therapy: toward combination strategies with curative potential. Cell 2015;161:205–14.
44. Deng L, Liang H, Xu M, Yang X, Burnette B, Arina A, et al. STING-dependent cytosolic DNA sensing promotes radiation-induced type I interferon-dependent antitumor immunity in immunogenic tumors. Immunity 2014;41:843–52.
45. Idzko M, Dichmann S, Ferrari D, Di Virgilio F, la Sala A, Girolomoni G, et al. Nucleotides induce chemotaxis and actin polymerization in immature but not mature human dendritic cells via activation of pertussis toxin-sensitive P2y receptors. Blood 2002;100:925–32.
46. Ma Y, Adjemian S, Yang H, Catani JP, Hannani D, Martins I, et al. ATP-dependent recruitment, survival and differentiation of dendritic cell precursors in the tumor bed after anticancer chemotherapy. Oncoimmunology 2013;2:e24568.
47. Golden EB, Frances D, Pellicciotta I, Demaria S, Helen Barcellos-Hoff M, Formenti SC. Radiation fosters dose-dependent and chemotherapy-induced immunogenic cell death. Oncoimmunology 2014;3:e28518.
48. de Leve S, Wirsdorfer F, Jendrossek V. Targeting the immunomodulatory CD73/adenosine system to improve the therapeutic gain of radiotherapy. Front Immunol 2019;10:698.
49. Jin D, Fan J, Wang L, Thompson LF, Liu A, Daniel BJ, et al. CD73 on tumor cells impairs antitumor T-cell responses: a novel mechanism of tumor-induced immune suppression. Cancer Res 2010;70:2245–55.
50. Lewis JE, Singh N, Holmila RJ, Sumer BD, Williams NS, Furdui CM, et al. Targeting NAD(+) metabolism to enhance radiation therapy responses. Semin Radiat Oncol 2019;29:6–15.

Published OnlineFirst February 11, 2020; DOI: 10.1158/2326-6066.CIR-19-0449

Cancer Immunology Research

CD73 Blockade Promotes Dendritic Cell Infiltration of Irradiated Tumors and Tumor Rejection

Erik Wennerberg, Sheila Spada, Nils-Petter Rudqvist, et al.

Cancer Immunol Res 2020;8:465-478. Published OnlineFirst February 11, 2020.

Appendix #2

Meeting abstract: 5th Annual Immuno-Oncology Young Investigators' Forum (IOYIF), Houston, Texas, USA, April 27, 2019

Adenosine generation in irradiated tumors represents a barrier to radiation-induced anti-tumor immunity

Erik Wennerberg PhD[1], Nils-Petter Rudqvist PhD[1], Claire Lhuillier PhD[1], Qiuying Chen PhD [2], Fengli Zhang PhD[2], Claire Vanpouille-Box PhD [1], Stephen S. Gross PhD [2], Silvia Chiara Formenti MD[1], Sandra Demaria MD PhD [1]

[1]Department of Radiation Oncology, Weill Cornell Medicine, New York, NY, USA.
[2]Department of Pharmacology, Weill Cornell Medicine, New York, NY, USA.

Tumor-targeted radiation therapy (RT) can promote systemic and tumor-specific immune responses in cancer patients that are unresponsive to immune checkpoint blockade (ICB) [1]. RT-induced production and release of nucleotides ATP and NAD by tumor cells contributes to the recruitment and activation of conventional type I dendritic cells (cDC1) to the tumor. cDC1 are uniquely capable of cross-presenting tumor antigens to CD8+ T cells, and essential for anti-tumor immune responses [2-4]. In the tumor microenvironment (TME), hydrolysis of ATP and NAD is mediated by CD39 and CD38, respectively, generating precursors for CD73-mediated adenosine production that has broad immunosuppressive effects on both cDC1 and CD8+ T cells [5].

In this study we tested the hypothesis that increased adenosine generation in the irradiated tumor hinders RT-induced anti-tumor immune responses.

Adenosine abundance was assessed by liquid chromatography-mass spectrometry (LC-MS) in subcutaneous TSA tumors. We assessed surface expression of CD73, CD38 and CD39 by flow cytometry on murine and human tumor cells 24 hours after RT-treatment. In order to assess the impact of CD73-mediated adenosine generation on the immunogenicity of 20Gy RT (previously shown ineffective at inducing recruitment of cDC1[6]), Wild type (WT) or BATF3-deficient ($BATF3^{-/-}$) mice (ablated development of cDC1) bearing subcutaneous TSA tumors were treated with 20Gy RT with or without concomitant CD73-blockade and monitored for tumor progression. Some mice were sacrificed 6 days after RT to analyze tumor-infiltrating DCs and T cells. Systemic anti-tumor effect of CD73-blockade was assessed by combined treatment with RT and anti-CTLA-4 in the rapidly metastatic mammary carcinoma model 4T1. Lung metastatic burden was assessed on day 28 after tumor inoculation.

In TSA tumors, adenosine concentration was significantly increased 24 hours after in vivo treatment with 20Gy single RT dose (**Figure 1**). In vitro, we demonstrated RT dose-dependent induction of CD73 and CD38 on TSA cells (**Figure 2**) which was confirmed in murine (4T1 and E0771) and human (MDA-MB-231 and 4175TR) breast cancer cells. CD39 was not detected on cancer cells but was expressed on tumor-infiltrating leukocytes. While CD73-blockade alone had no significant effect on tumor progression, in mice treated with 20Gy RT, CD73-blockade improved significantly RT-induced tumor control, an effect associated with enhanced recruitment of cDC1 and CD8+ T cells to

the tumor. Consistent with the hypothesis that cDC1 are essential for RT-induced anti-tumor responses, the improved tumor response obtained with RT and CD73 blockade was abrogated in BATF3-/- mice (**Figure 3**). Recruitment of DC to irradiated tumors in the presence of CD73 blockade was confirmed in adoptive transfer experiments. Importantly, CD73-blockade in combination with ICB and RT induced systemic anti-tumor immune responses inhibiting lung metastases in the 4T1 model (**Figure 4**).

Our findings show that 20Gy RT upregulates expression of ectoenzymes in the non-canonical pathway of extracellular nucleotide catabolism promoting adenosine accumulation in the irradiated tumor. Blocking adenosine generation by CD73-blockade is a promising therapeutic approach to enhance systemic tumor responses to the combination of RT and ICB. Agents targeting CD73 are currently in clinical testing, thus this approach could be rapidly translated to the clinic.

Figure 1. Average adenosine ion abundance in TSA tumors. BALB/c mice bearing subcutaneous TSA tumors were treated with local RT delivered as 0, 8, 12 or 20 Gy. 24 hours after RT-treatment, tumors were excised and adenosine abundance was measured using liquid chromatography-mass spectrometry (LC-MS).

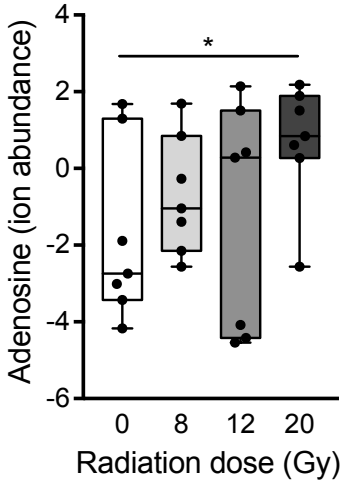

Figure 2. Surface expression of CD73 and CD38 on TSA cells 24 hours following RT. Graph depicts fold change in MFI compared to mock-treated cells (0 Gy).

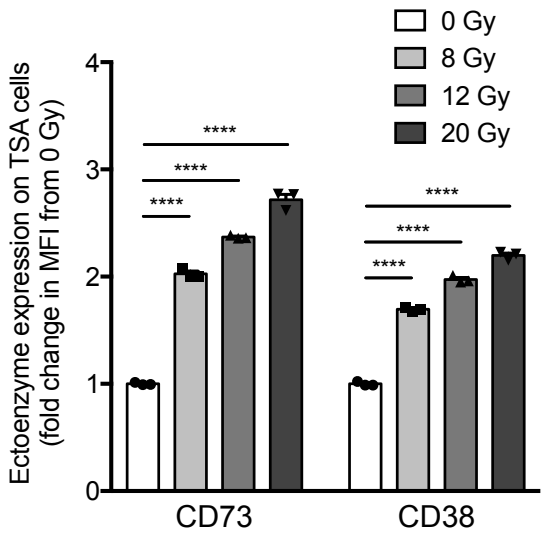

Figure 3. Progression of TSA tumors in WT or BATF3$^{-/-}$ mice. TSA tumors were injected subcutaneously on day 0 and assigned to treatment with: 0Gy + isotype control antibody (iso ctrl), 0Gy + anti-CD73 (aCD73), 20Gy + iso ctrl and 20Gy + aCD73. aCD73 (TY/23, 100 µg) was administered i.p. on day 11, 14, 17 and 20. RT was given locally to the tumor as single 20Gy dose on day 12. Two-way ANOVA was used to calculate statistical differences in tumor progression. **p<0.01

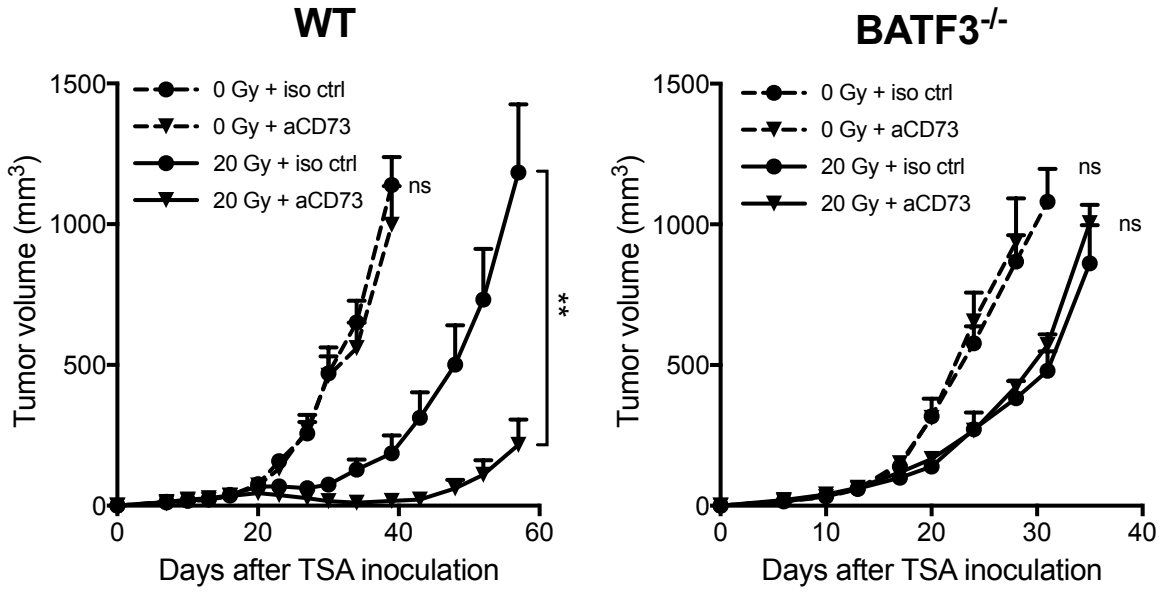

Figure 4. Lung metastasis count on day 28 after primary 4T1 tumor inoculation. BALB/c mice bearing subcutaneous 4T1 flank tumors were either mock-treated (0Gy) or treated with 20 Gy RT at day 11. Mice received aCD73 mAb on day 10, 13, 16 and 19 and/or aCTLA-4 on day 11, 14 and 17

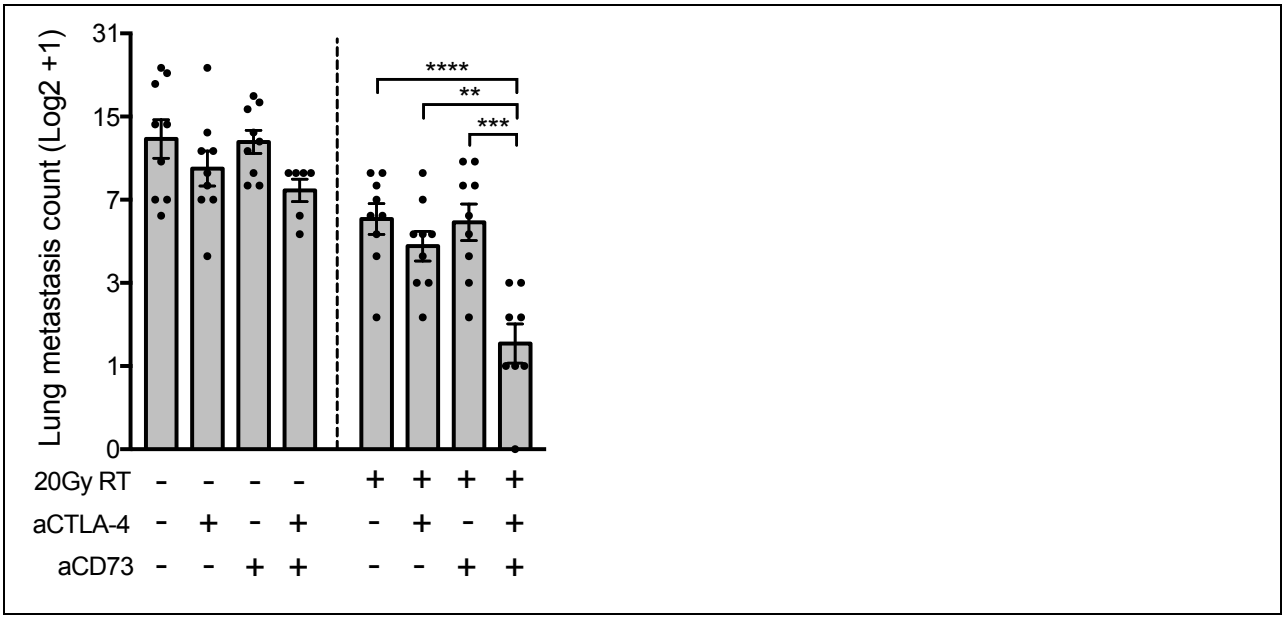

1. Formenti, S.C., et al., *Radiotherapy induces responses of lung cancer to CTLA-4 blockade.* Nat Med, 2018. **24**(12): p. 1845-1851.
2. Ma, Y., et al., *ATP-dependent recruitment, survival and differentiation of dendritic cell precursors in the tumor bed after anticancer chemotherapy.* Oncoimmunology, 2013. **2**(6): p. e24568.
3. Haag, F., et al., *Extracellular NAD and ATP: Partners in immune cell modulation.* Purinergic Signal, 2007. **3**(1-2): p. 71-81.
4. Golden, E.B., et al., *Radiation fosters dose-dependent and chemotherapy-induced immunogenic cell death.* Oncoimmunology, 2014. **3**: p. e28518.
5. Chen, L., et al., *CD38-Mediated Immunosuppression as a Mechanism of Tumor Cell Escape from PD-1/PD-L1 Blockade.* Cancer Discov, 2018. **8**(9): p. 1156-1175.
6. Vanpouille-Box, C., et al., *DNA exonuclease Trex1 regulates radiotherapy-induced tumour immunogenicity.* Nat Commun, 2017. **8**: p. 15618.

Appendix #3

Meeting abstract: 5th CRI-CIMT-EATI-AACR International Cancer Immunotherapy Conference (CICON), Paris, France, September 25 - 28, 2019.

CD73 blockade potentiates radiation-induced tumor infiltration of conventional type I dendritic cells and abscopal anti-tumor effects in combination with immune checkpoint blockade

Erik Wennerberg PhD[1], Nils-Petter Rudqvist PhD[1], Claire Lhuillier PhD[1], Qiuying Chen PhD [2], Fengli Zhang PhD[2], Xi Kathy Zhou[3], PhD, Claire Vanpouille-Box PhD [1], Steven S. Gross PhD [2], Silvia Chiara Formenti MD[1], Sandra Demaria MD PhD [1]

[1]Department of Radiation Oncology, Weill Cornell Medicine, New York, NY, USA.
[2]Department of Pharmacology, Weill Cornell Medicine, New York, NY, USA.
[3]Department of Healthcare Policy and Research, Weill Cornell Medicine, New York, NY, USA

Tumor-targeted radiation therapy (RT) can promote systemic and tumor-specific immune responses in cancer patients that are unresponsive to immune checkpoint blockade (ICB). RT-induced danger signals including release of nucleotides ATP and NAD by tumor cells contribute to tumor infiltration and activation of conventional type I dendritic cells (cDC1), which are uniquely capable of cross-presenting tumor antigens to CD8+ T cells, and essential for anti-tumor immune responses. In the tumor microenvironment (TME), hydrolysis of ATP and NAD, mediated by CD39 and CD38 respectively, generates precursors for CD73-mediated adenosine production that has broad immunosuppressive effects on both cDC1 and CD8+ T cells. In the present study, we tested the hypothesis that adenosine generation in irradiated tumors hinders RT-induced cDC1 infiltration and anti-tumor immune responses.

Tumor adenosine levels were assessed by liquid chromatography-mass spectrometry (LC-MS) in subcutaneous TSA mouse tumors and surface expression of CD73, CD38 and CD39 was measured by flow cytometry on murine (TSA and 4T1) and human (MDA-MB-231 and 4175TR) tumor cells. In order to assess the impact of CD73-mediated adenosine generation on the immunogenicity of 20Gy RT (previously shown ineffective at inducing cDC1 tumor infiltration), Wild type (WT) or BATF3-deficient ($BATF3^{-/-}$) mice (ablated development of cDC1) bearing subcutaneous TSA tumors were treated with 20Gy RT with or without concomitant CD73-blockade (anti-CD73 monoclonal antibody, TY/23) and monitored for tumor progression. Some mice were sacrificed 6 days after RT to analyze tumor-infiltrating DCs and T cells. cDC1s, generated from bone marrow cells cultured with FLT3L and GM-CSF, were CFSE-labeled and administered intravenously in mice bearing irradiated flank TSA tumors and contralateral non-irradiated tumors. Tumor infiltration of labeled cDC1s was assessed after 48 hours by flow cytometry. Systemic anti-tumor effect of CD73-blockade was assessed by combined treatment with RT and anti-CTLA-4 in the rapidly metastatic mammary carcinoma model 4T1. Lung metastatic burden was assessed on day 28 after tumor inoculation.

In TSA mouse tumors, a single dose of 20Gy RT significantly elevated adenosine levels after 24 hours. In vitro, CD73 and CD38 expression on murine and human breast cancer cells was increased following RT. CD73-blockade alone had no significant effect on tumor progression. However, in mice

treated with 20Gy RT, CD73-blockade improved significantly RT-induced tumor control and mouse survival, an effect associated with enhanced tumor infiltration of activated cDC1 and CD8 T cells. Consistent with the hypothesis that cDC1 are essential for RT-induced anti-tumor responses, the observed synergy between RT and CD73 blockade was abrogated in BATF3-/- mice. Improved infiltration of cDC1 in irradiated tumors of anti-CD73-treated mice was confirmed in adoptive transfer experiments of *ex vivo* generated cDC1. Importantly, we observed that CD73-blockade in combination with ICB and RT induced systemic anti-tumor effects in the 4T1 model, reducing lung metastasis burden compared to RT, ICB or anti-CD73 alone.

Our findings show that RT upregulates expression of ectoenzymes in the non-canonical pathway of extracellular nucleotide catabolism promoting adenosine accumulation in irradiated tumors. We demonstrate that CD73 blockade can synergize with tumor-targeted RT to promote tumor infiltration of cDC1, primary tumor control and potentiate abscopal tumor effects in combination with ICB. With CD73 blocking antibodies currently in clinical testing, implementation of CD73 blockade with radiotherapy/immunotherapy combinations represents a promising treatment option to improve responses in ICB refractory cancer patients.